NON-MODEL BASED ADAPTIVE CONTROL OF RENEWABLE ENERGY SYSTEMS

by

FARYAD DARABI SAHNEH

B.S., Amirkabir University of Technology, Iran, 2008

A THESIS

submitted in partial fulfillment of the
requirements for the degree

MASTER OF SCIENCE

Department of Mechanical and Nuclear Engineering
College of Engineering

KANSAS STATE UNIVERSITY
Manhattan, Kansas
2010

Approved by:

Major Professor
Guoqiang Hu

Copyright

Abstract

In some types of renewable energy systems such as wind turbines or solar power plants, the optimal operating conditions are influenced by the intermittent nature of these energies. This fact, along with the modeling difficulties of such systems, provides incentive to look for non-model based adaptive techniques to address the maximum power point tracking (MPPT) problem. In this thesis, a novel extremum seeking algorithm is proposed for systems where the optimal point and the optimal value of the cost function are allowed to be time varying. A sinusoidal perturbation based technique is used to estimate the gradient of the cost function. Afterwards, a robust optimization method is developed to drive the system to its optimal point. Since this method does not require any knowledge about the dynamic system or the structure of the input-to-output mapping, it is cosidered to be a non-model based adaptive technique. The proposed method is then employed for maximizing the energy capture from the wind in a variable speed wind turbine. It is shown that without any measurements of wind velocity or power, the proposed method can drive the wind turbine to the optimal operating point. The generated power is observed to be very close to the maximum possible values.

Table of Contents

List of Figures

List of Tables

Acknowledgments

Foremost, I would like to especially thank my advisor Dr. Hu for his continuous support during my study at Kansas State University. I am truly grateful for all his contributions to make my experience at K-state very fruitful. With his enthusiasm and dedication, he instilled in me the passion to excel. This research would not have been possible without his contributions of time, ideas, and sound advice. I would also like to thank him for his suggestions, corrections and upgrades to this manuscript.

I was highly pleased to interact with Dr. Schinstock and Dr. White by attending their classes and having them as my committee members. I also wish to thank them for their time and effort reviewing my thesis manuscript and providing me with their constructive comments and inputs to improve this work.

My warm thanks are due to my fellow labmates at Smart Autonomous Systems and Control Lab: Tony Hawkins, Joshua Cook, and Yang Wang for their friendship, collaboration, and all the fun we had through past two years. I wish to thank my colleagues, friends, and other faculty members at K-state for helping me getting through hard times and for all the support and camaraderie they provided.

Finally, there are not enough words to thank my family and especially my wife, Ala, for their unconditional and unending support and encouragement throughout my work.

Dedication

To my beloved wife, Ala, for her endless love, patience, and support.

Chapter 1

Introduction and Problem Statement

1.1 Introduction

Wind energy is currently the fastest-growing source of electricity in the world (Laks et al. 2009). Wind provides the energy industry with a clean and viable alternative for the generation of electric power. However, the portion of the energy generated by wind turbines is currently limited due to several issues regarding the implementation and integration with other resources. A good overview of the recent developments in advanced controllers for wind turbines and wind farms as well as the open problems in the area of modeling and control of wind turbines can be found in Pao and Johnson 2009. Control problems associated with wind turbines can basically be categorized into three levels. The first level involves the control goal of capturing the maximum power from the wind turbine while decreasing the stress and mechanical loads on the wind turbine. The second and third levels are the farm level and the grid level, respectively. The control problems in these levels lie beyond the scope of this study which focuses specifically on the power capture problem and is the subject of this thesis.

One type of wind turbines that demonstrates great efficiency is the variable-speed wind turbine. Variable-speed wind turbines have three main regions of operation. Region 1 is where the wind speed is too low and no power is generated; region 2 is an operational mode during which it is desirable to capture as much power as possible from the wind; region 3

occurs to when the wind speed is so high that the turbine must limit the fraction of the captured power to ensure safe electrical and mechanical loads (Johnson et al. 2004).

Before discussing the existing control strategies for maximum power point tracking (MPPT) problem, it is important to identify the key issues which must be considered for the control algorithm design. 1) Modeling the aerodynamic effects of wind is almost impossible due to the turbulent nature of wind. Moreover, a precise model of a wind turbine is hard to develop. 2) Although several technologies for measuring wind velocity exist, it is not possible to have accurate measurements. This fact makes a control algorithm with little or no dependency on wind measurements very interesting, from both technological and commercial points of view. 3) Similar to wind velocity, direct measurements of captured power is challenging; this factor specifically limits the application and performance of maximum power point tracking algorithms. 4) The optimal operating points in a wind turbine are not known because they highly depend on the wind turbine structure, installment, and the atmospheric conditions. 5) The time varying nature of wind induces a time varying characteristic to the optimal operating points. This issue necessitates that the developed control strategy can identify the optimal points online. 6) According to technological and commercial restrictions, consideration of mechanical stress, load, and fatigue during operation is crucial. (see Chen and Spooner 2001 and Rodriguez-Amenedo et al. 2002)

This chapter is organized as follows. Section 1.2 provides a brief review of modern energy systems to provide a broader view of control problems in this area. In section 1.3, the problem addressed in this thesis is introduced and discussed. An overview of the thesis and the contributions are provided in section 1.4.

1.2 Background on Modern Energy Systems and Motivation

Power infrastructure is an indispensable element of modern society. Policies towards reducing the impacts of global climate change, shortages of traditional energy resources, and the

need for greater energy security have made the power industry face the largest challenges in its history. A revolution with the goal of transition to more secure, sustainable and affordable energy future is happening. Many national and international companies, as well as research centers are invested in the common goal of revolutionizing the energy industry. Consequently, a promising opportunity exists for researchers in the academic environment. The following section identifies the dominant trends in power systems and lists some control problems related to this area.

1.2.1 Trends in Power Systems

In this section three substantial trends in power systems are reviewed. First, the power industry is commercializing the generation of power from renewable sources. Second, there is a tendency towards distributed generation in which the power is generated close to the consumer. Third, the tremendous advances in information technology are being utilized to develop a reliable and intelligent power infrastructure.

1.2.1.1 Emergence of Renewable Energy

Conventionally, energy has been generated from fossil fuels and coal. Issues such as pollution, availability, and generation costs, compounded by the increasing demand for energy are forcing the energy industry to seek and achieve integration of new alternative energies. Renewable energy sources may provide viable solutions due to their ubiquitousness and clean nature. Accordingly, renewable energy sources have gained substantial attention in recent decades. Many countries, particularly European countries and the United States, are investing large amounts of money to enhance and develop several types of renewable energies and corresponding technologies. Wind power, solar energy, hydropower, biomass, biofuel, and geothermal energy are considered to be the main renewable sources of energy. Despite all the advantages these clean energies present, there are still several issues and constraints regarding implementation and integration of renewable energies. For example, the intermittent nature of wind power has made the integration of wind turbines to the

main electric grid a very serious problem for the wind industry.

1.2.1.2 Distributed Generation

The second trend emerges from the tendency toward distributed generation (Ackermann et al. 2001). There are three main steps in a power generation system. Power is first generated at a power plant. Then, it is transferred to the place where it will be used. Finally, it is distributed among consumers. In conventional power systems, electricity is generated in large centralized power plants. This kind of generation is very economical but there are several shortcomings with the transmission and distribution process (Rabinowitz 2000). Transmission is very expensive, has harmful environmental effects, and distribution is very inefficient. Recently, distributed generation is proposed as a reliable and economical approach to the whole power process. In a distributed generation architecture, electricity is generated in small scale facilities very close to the place of consumption. This approach dramatically decreases costs associated with transmission and distribution. The small scale distributed power generation sites are mostly connected together in larger grid and consequently to the bulk grid. In this case, the power infrastructure will be a large-scale grid which is geographically distributed (see, Hammons 2008, Lasseter and Paigi 2004, Coll-Mayor et al. 2004). This type of grid requires more advanced technologies in management, control, and communication than those currently used in conventional power infrastructure.

1.2.1.3 Information-Rich Grids

Over the past few decades, advances in communication and information technologies have dramatically impacted the world in almost every respect. Like any other industry, the power industry is trying to realize the potentials of utilizing information technologies. In fact, current topics of power systems such as smart grid and wide area generation mainly rely on information advances. Future power systems and their corresponding departments are moving towards thorough networking of stations, associations, and corporations to enable an intelligent power infrastructure to be feasible (Rabinowitz 2000). Consequently, this will

result in more secure and reliable generation, transition, and distribution. The goals of the information architecture cannot be achieved unless synchronous monitoring, ample data collection, information communication, and online processing are all performed successfully. It should be noted that although these factors are integral parts of a system, each one comprises a separate ongoing research topic.

1.2.2 Selected Control Problems in Modern Power Systems

In this section, some problems in modern power systems are listed which are important to the control academic society.

1.2.2.1 Maximum Power Point Tracking

One of the extremely desirable factors for any energy system is for it to operate at the optimal conditions. In an intermittent energy source, the optimal operating points are constantly changing. Therefore, some kinds of mechanisms are required to rapidly track the optimal operating points of the system. This topic is referred to as the *maximum power point tracking* (MPPT) problem in power systems. It should be noted that MPPT mechanism is totally separate from the mechanical approaches designated for the same goal (dan Zhong et al. 2008). For instance, in photovoltaic systems there is a mechanical mechanism that makes the cells track the position of the sun so that it is always perpendicular to the sunlight. The online identification an tracking of the optimal operating points are crucial. An MPPT mechanism that is simple and low cost, has quick tracking under changing conditions, and ensures small output power fluctuation is highly desirable (Salas et al. 2006).

1.2.2.2 Connection to the Grid

During the past decades, renewable energy sources have been mostly limited to small scale applications. Therefore, it was somewhat acceptable to ignore the impact of connecting renewable energies to the power grid (Zavadil et al. 2005). As discussed earlier, trends in energy systems are moving toward the use of more renewable sources of energy. Hence, a

noticeable portion of the generated energy will be that of renewable sources. Consequently, understanding of potential impacts of interaction between wind turbine plants and the bulk power system is necessary. This problem deals with a highly nonlinear dynamic system with a number of uncertainties and disturbances. Therefore, nonlinear, robust, or adaptive control methods are good candidates for the control approach.

1.2.2.3 Decentralized Control of a Power Grid

Power systems are viewed as multi-input/multi-output systems with super-high dimensionality as well as many nonlinearities and uncertainties which are geographically distributed over wide areas. The ideal scenario for control of power systems would consist of a central decision-making station which can drive the system to the optimal operating conditions. In this scenario, all the required information about the power system and the grid topology should be instantly available to the central station. In addition, the central station should be able to process the huge amount of collected data and solve for a multi-objective optimization problem. With the current technology, a central scenario such as this is not possible and decentralized schemes for control and optimization seem to be the only possible alternative. Instead of centrally-coordinated decision schemes, the subsystems may be viewed as agents in a multi-agent system with different cooperative or competitive objectives, depending on the system-wide objectives and the structure of the system.

1.2.2.4 Control Over Networks in Power Systems

Future power infrastructure networks will consist of several layers including physical power layer, service, information, and decision layers. This multi-layer network enables full control over the whole infrastructure. In these multi-layer networks, communication and connections will be conducted through both the individual layer as well as the inter-layer links. It is not difficult to imagine how vital the network management task will be for such systems. Here, it is worthwhile to note the difference between network control and control over network. A network, such as the internet, requires to control and management to function. On the

other hand, it is possible to utilize the communication capabilities of an information network to allow control loops. Imagine data collection at a location through sensors. Then, the collected data is transferred to another site in order to be processed. An appropriate decision is made and sent out to the actuators which may be located at a different place. This whole procedure is referred to as control over network. As mentioned earlier, control over network is a hot topic in controls area. It is obvious that a sophisticated network like that of power infrastructure can be a very interesting and also a challenging opportunity for control researchers to work on.

1.3 Problem Statement

In this thesis, the maximum power point tracking problem for a wind turbine system is addressed. As mentioned in Section 1.2.2.1, the MPPT is particularly required to have the capability to identify and track the trajectory of the optimal point. Since the wind velocity is constantly changing, the optimal rotor speed also varies. Furthermore, the maximum power which can be captured depends on the wind velocity which is time-varying. Taking into account the difficulty of wind velocity measurements and aerodynamic modeling of the wind, it is very challenging to track the optimal operating point of the wind turbine system. Below is the problem addressed in this thesis report.

Problem I: Consider a variable speed wind turbine and assume that the aerodynamic interaction between the wind field and the turbine structure is poorly modeled. In addition, the wind field conditions are constantly changing. Assume that there is no reliable measurements of the wind velocity available. Design a maximum power point tracking algorithm that has the capability to identify and track the trajectory of the optimal rotor speed.

One class of adaptive control methods is called extremum seeking control (ESC). Extremum seeking control algorithms are non-model based adaptive techniques which can identify the optimum point of an unknown mapping. In extremum seeking control, the states of a dynamic system are regulated to a point where cost function is maximized (or

minimized). ESC methods have been proposed for addressing several practical problems, including the MPPT problem. Specifically, the ESC methods have been very successful for the MPPT problem in photovoltaic plants (Brunton et al. 2009). Particularly for systems like wind turbines in which the aerodynamic interaction between wind and the turbine structure is unknown, the ESC control methods can be a good candidate for addressing the MPPT problem. However, there is one issue with wind turbines which tests the possibility of application of conventional ESC methods. The current ESC methods are mostly used for mappings with no dependency on time. However, persistent variations in wind velocity and wind field conditions renders the power map time dependent. As a result, stable application of current ESC methods to the MPPT problems demand long run averaging of the power mapping. Consequently, efficiency is affected. A generalization of extremum seeking control methods to address time-varying mappings is a promising development.

Problem II: Design an ESC algorithm for unknown time dependent input-to-ouput mappings. The optimal point of the mapping is also time varying. The time variation structures of the mapping and the optimal point are also unknown. Like other ESC methods, only the measurements of the mapping is available for the feedback purpose.

In the extremum seeking literature, there are some results for time-varying mappings (see Ariyur and Krstic 2003). However, the variation is restricted to a very specific structure. In addition, the time-dependency should be known. Therefore, designing an extremum seeking algorithm where the mapping is time-dependent in a general form is an improvement on previous results. As will be discussed later, such extremum seeking methods can be very useful for the MPPT problem in wind turbines.

In Chapter 2, an overview of extremum seeking methods is provided. Chapter 3 is devoted to designing the ESC algorithm in Problem II. This ESC algorithm is then employed in Chapter 4 to address the main MPPT problem introduced in Problem I.

1.4 Contributions and Thesis Overview

In this thesis, variations in the mapping are handled in the following approach. The variation of the optimal point is treated as a smooth disturbance. The disturbance is identified using a robust identifier and then a gradient search law is introduced which can asymptotically converge to a time-varying optimum. The RISE gradient search law requires that the gradient be known. The gradient is generated directly through sinusoidal perturbations and a delay-based demodulator. An extremum seeking control algorithm is then built based on the assumption that time scales for plant dynamics, sinusoidal perturbation, and the adaptation dynamics are separate. The designed ESC algorithm is then applied to the MPPT problem in wind turbines.

The contribution of the current work is two-fold. First, the results in extremum seeking control methods are extended to consider general time varying mappings. Second, the proposed MPPT algorithm eliminates any unnecessary reliance on exact modeling of the wind turbine system or wind velocity measurements. Since the proposed ESC method is primarily designed for time-varying mappings, there is no need to use averaged power mapping. This fact increases the efficiency of the MPPT method while maintaining the robustness and stability of the closed loop system.

Chapter 2

Extremum Seeking Control Method

2.1 Introduction

The objective of many control problems is to regulate the output of a dynamic system at a prescribed set point or to track a prescribed trajectory. Accordingly, the mainstream developments in linear, nonlinear, and adaptive control theories seek to achieve the same objectives. However, in many control applications, the desired set point or trajectory is not known and must be determined so that the output of the dynamic system reaches its extremum (i.e., maximum or minimum) value. This class of control problems is known as *extremum seeking control (ESC)* or *self-optimizing control* and the corresponding theory is categorized as adaptive control methods (see, Krstic and Wang 2000, Tan et al. 2009, Tan et al. 2008, Ariyur and Krstic 2004, Krstic 2000, Manzie and Krstic 2009, Ariyur and Krstic 2003, and the references therein). Extremum seeking control is a non-model based[1] gradient search method that dynamically seeks the optimal point of the input-output mapping of a system. Being non-model based by nature makes these methods robust to modeling, which is very appealing for many practical applications.

During the 1950's and 60's (much earlier than the emergence of adaptive control theory), ESC methods were very popular among control researchers and provided noticeable appli-

[1] In the literature, there exists some model-based methods which are also referred to as extremum seeking control. For more information on these methods, please refer to Guay and Zhang 2003. These methods are not discussed in this report.

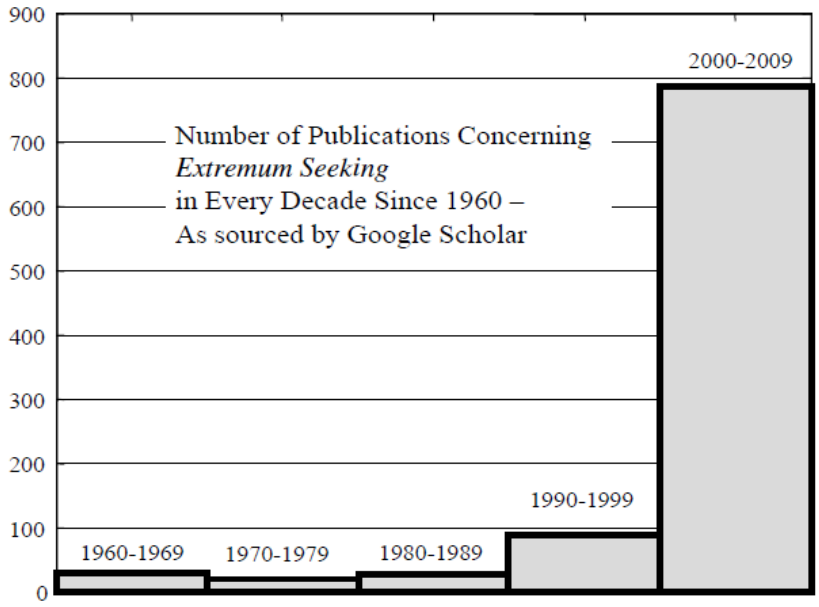

Figure 2.1: *Time line of extremum seeking publications (Tan et al. 2010)*

cation in many practical problems. This interest was soon abandoned because no precise stability analysis could be found despite all the efforts at that time. Several years later, Krstic and Wang 2000 provided the first rigorous stability analysis for a class of ESC control problems through singular perturbation theory and averaging method. After their 2000 paper, the control community showed a renewed interest in ESC. As can be seen in Fig. 2.1, the number of publications on ESC experiences a jump after 2000. More information about the extremum seeking control method may be found in the recent survey paper Tan et al. 2010.

Consider the dynamic system:

$$\begin{aligned} \dot{x} &= f(x,u) \\ y &= h(x), \end{aligned} \tag{2.1}$$

where $x \in \mathbb{R}^n$ is the state, $u \in \mathbb{R}^m$ is the control input, $y \in \mathbb{R}^r$ is the output. The functions $f(x,u)$ and $h(x)$ determine the system dynamics and output, respectively.

Consider the following two problems:

Problem 1. Design the control input u such that the state x regulates at the set point x_0.

This problem is known as the regulation problem. There exists extensive results for this problem in the literature. If the measurements of x are available for feedback, the problem is specified as state feedback regulation. If only measurements of y are available, the problem is known as output feedback regulation.

Problem 2. Design the control input u such that the state x regulates at the point x^* where $y^* = h(x^*)$ is at its maximum value. The function $h(x)$ is *unknown*.

It is not possible to readily provide a closed loop solution to this problem. As can be realized from the problem statement, this problem is a combination of regulation and optimization problems. The question becomes how to formulate the problem so that the extensive results in regulation problem and optimization techniques can be used. This problem is known as the extremum seeking control problem in the literature.

The idea of extremum seeking control begins with introducing a new state θ to the system. The extremum seeking problem would then be split into two parts. 1) Regulation of x at $l(\theta)$, where $l(.)$ is a real function. 2) Optimization search for θ to converge to θ^*, where y^* is at its extremum (i.e. maximum of minimum) value. However, one might question how these two processes are coupled.

2.2 Structure of Extremum Seeking Algorithms

A typical extremum seeking control loop consists of three major components, as illustrated in Figure (2.2). The first component is the mapping, which maps the input θ to the output y. The system to be controlled is embedded in the mapping. The second component is responsible for the gradient estimation. In this component, the measurements of output y is utilized to estimate the gradient of the mapping with respect to θ. The final component uses the estimated gradient to perform an optimization search. In the following section, these three main components of an extremum seeking loop are discussed in greater detail.

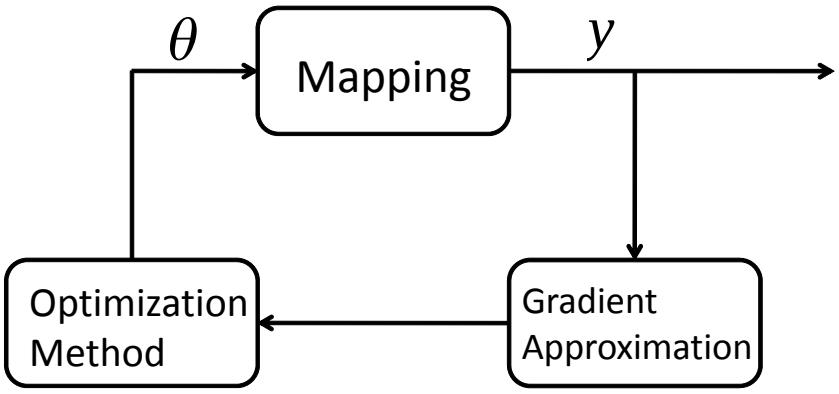

Figure 2.2: *Schematic of the structure of extremum seeking methods*

The arguments provide some insights for understanding the underlying logic of extremum seeking control and facilitate a comparative study of different ESC methods.

2.2.1 Mapping

The mapping relates the parameter θ to the output y. There are several aspects involved in categorizing the mapping, including the mapping function structure, the dynamical characteristic of the mapping, and time dependency. These aspects are used to give a precise definition of the mapping in the analysis. These aspects are studied in greater detail.

Mapping Function Structure: A mapping should have an extremum point for the ESC problem to make sense. Mostly, it is assumed that the mapping has a single optimal point, however, a case with multiple local extrema was recently studied in Tan et al. 2009. In addition, the mapping is assumed to be a smooth function of θ. Being smooth is not a necessary condition for having an extremum but it makes the analysis much more straight forward. A typical mapping is assumed to have the following form (Ariyur and Krstic 2003)

$$y = Q(\theta) = Q^* + Q^*_{\theta\theta}(\theta - \theta^*)^2, \tag{2.2}$$

at least locally. The conditions for a non-local analysis has been stated as

$$Q(\theta^*) = 0,\ Q_{\theta\theta}(\theta^*) < 0 \tag{2.3}$$

$$Q_\theta(\theta^* + \xi)\xi < 0,\ \forall \xi \neq 0. \tag{2.4}$$

Note that condition (2.3) is the necessary condition to have a maximum for a smooth function. Condition (2.4) is a sufficient condition for having a single maximum point (Tan et al. 2006).

Dynamical Characteristics: As discussed earlier, the mapping embeds the regulation process. In this context, the mapping from θ to $Q(\theta)$ is always dynamic in practice. However, for the analysis, the mapping can be considered static with the assumption that the regulation is much faster than the adaptation process for the parameter θ. In other words, the regulation process is assumed instantaneous. A general nonlinear mapping was rigorously analyzed in Krstic and Wang 2000 where the system mapping has the following form

$$\begin{aligned} \dot{x} &= f(x, u) \\ y &= h(x), \end{aligned} \tag{2.5}$$

and $u = \alpha(x, \theta)$ exponentially regulates the system states at $x = l(\theta)$. The plant had to be very fast (quasi-static). The authors used a singular perturbation analysis to go from a quasi-static mapping to a static mapping. Krstic 2000 extended the results for static and quasi-static input-to-output mappings by considering input and output dynamics. A mapping of the form $F_i(s)Q(\theta)F_o(s)$ is considered, where $F_i(s)$ and $F_o(s)$ are the input and the output dynamics which are exponentially stable and proper. The proposed algorithm benefits from designing a dynamic compensator in the control loop.

Time Dependency: The optimal points of a mapping can be constant or time-varying. Almost all of the results in the literature concern a case where the optimal point and the optimal value are constant through time. Correspondingly, these methods are suitable only

for systems where the variations of the mapping are very slow. Krstic 2000 considered time-varying mappings where the structure of the variation through time is known, namely,

$$\mathcal{L}(\theta^*(t)) = \lambda_\theta^* \Gamma_\theta(s) \tag{2.6}$$

$$\mathcal{L}(Q^*(t)) = \lambda_Q^* \Gamma_Q(s) \tag{2.7}$$

where $\Gamma_\theta(s)$ and $\Gamma_Q(s)$ are *known* transfer functions and λ_θ^* and λ_Q^* are unknown constants. To date, no results have been reported for the general case of time dependent mappings. In this thesis report, the existing assumptions about the time dependency of the mapping are removed and results are provided for time dependent mappings in a very general form.

2.2.2 Gradient Approximation

There are several methods for approximating the gradient when only the input-to-output mapping is available. The simplest numerical method for approximation of the gradient is the finite difference method. In this method, a perturbation is applied to one variable and then the corresponding gradient value is approximated by measuring the rate of change of the output with respect to the applied perturbation. The finite difference method gives a very good approximate of the gradient vector. However, for an N dimensional state, the finite difference method requires $2N$ measurements to compute the gradient vector. This requirement increases the computation cost and limits the application of this method. Another similar method is called Finite Difference Stochastic Perturbation (FDSA). In this method, all the components of the state are perturbed at the same time in a random direction. Therefore, regardless of the dimension of the state, this method requires only two measurements for gradient approximation. The approximated gradient is less accurate than the one from the finite difference method. However, it is shown that in a gradient search the approximation is unbiased.

In continuous time extremum seeking methods, use of dither signal for gradient approximation is very common. Among different possible types of dither signals, sinusoidal

and stochastic perturbation are more popular. Sinusoidal perturbation method for gradient approximation is used in this thesis.

2.2.3 Optimization

The easiest optimization method is the steepest descent, expressed in the following form

$$\theta_{k+1} = \theta_k + \epsilon \hat{g}_k, \tag{2.8}$$

where $\hat{g}_k$ is the estimate of the gradient vector at time step k and ϵ is the search update rate. The continuous version of the steepest descent optimization method is commonly used in most of the extremum seeking algorithms, which has the following form

$$\dot{\theta} = \alpha \hat{g}(t). \tag{2.9}$$

There is also much literature on the nonlinear programming optimization methods. Some nonlinear programming methods have the capability of optimizing when noisy measurements of the input-output mapping are available. Teel and Popovic 2001 made use of this idea for developing extremum seeking algorithms and the consequent analysis.

2.3 How an Extremum Seeking Control Method Works

2.3.1 Introduction

A typical extremum seeking control problem has the following form. Consider a general nonlinear system of the form (2.1). Assume that a control law

$$u = \alpha(x, \theta) \tag{2.10}$$

is available which asymptotically stabilizes (2.1) at

$$x = l(\theta). \tag{2.11}$$

The design of a strategy to drive θ to the optimal points θ^*, such that $y = Q(\theta)$ is at its extremum value is desired, where $Q(\theta)$ is defined as the composition of $h(\cdot)$ and $l(\cdot)$, i.e.,

$$Q(\theta) \triangleq hol(\theta). \tag{2.12}$$

In this section, two extremum seeking algorithms which are different in nature are considered and the idea of why each algorithm works is discussed. The goal of this section is to examine the idea behind the ESC algorithms rather than to investigate them in full.

2.3.2 Extremum Seeking Control Based on Numerical Optimization Method

Numerical methods for optimization are basically discrete. In methods of extremum seeking control based on numerical optimization, the control approach is as follows:

1. Select a *suitable* θ_0 and set $k = 0$.
2. Use a controller that asymptotically regulates the system state at $x_k = l(\theta_k)$.
3. Wait until state x is *sufficiently* regulated at $l(\theta_k)$. At this point, the output $\hat{h}(x_k)$ is measured.
4. Use a numerical optimization technique to find θ_{k+1} according to the values of θ_i and the outputs $\hat{h}(x_i)$, $i = 0, ..., k$. Increase k to $k + 1$.
5. Continue to step 2.

Remark 1. *During the regulation process in step 3, x will not exactly equal $l(\theta_k)$. As a consequence, the measured output will be slightly different from $h(x_k) = Q(\theta_k)$. The longer the regulation process, the more accurate the estimates. However, devoting a long time to regulation for each update will increase the extremum seeking run time. Methods of nonlinear programming can be used to overcome this issue (Teel and Popovic 2001). Several nonlinear programming methods can solve the optimization problem even with measurement errors on the output. By devoting less time to the regulation process, the resultant errors can be considered as noise on the measurements. Hence, the extremum seeking convergence rate is enhanced.*

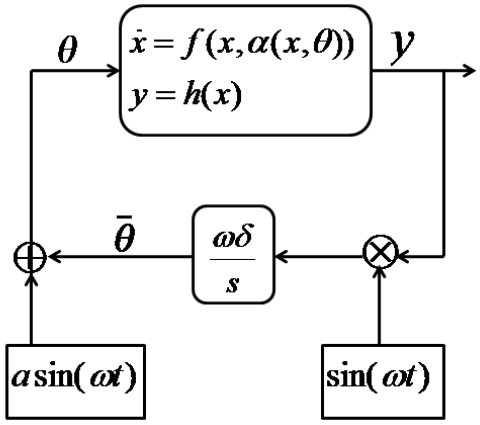

Figure 2.3: *First order extremum seeking algorithm (Tan et al. 2006).*

2.3.3 Continuous Time Extremum Seeking Control Based on Sinusoidal Perturbation

A schematic of the first order extremum seeking control algorithm is depicted in Figure (2.3). The analysis is based on the singular perturbation method and averaging method.

The first order extremum seeking algorithm can be written in the following closed form

$$\begin{aligned} \dot{x} &= f(x, \alpha(x, \bar{\theta} + a\sin(\omega t))) \\ \dot{\bar{\theta}} &= \omega\delta h(x)\sin(\omega t). \end{aligned} \tag{2.13}$$

The closed loop system (2.13) will be in the form of a standard singular perturbation problem (see Khalil 2002) by defining $\sigma = \omega t$, i.e.

$$\omega\frac{dx}{d\sigma} = f(x, \alpha(x, \bar{\theta} + a\sin(\sigma))) \tag{2.14}$$

$$\frac{d\bar{\theta}}{d\sigma} = \delta h(x)\sin(\sigma) \tag{2.15}$$

According to the standard singular perturbation method, the dimension of the state space is reduced by setting $\omega = 0$ in the equation (2.14). Therefore, the differential Eq. (2.14) becomes an algebraic equation:

$$f(x, \alpha(x, \bar{\theta} + a\sin(\sigma))) = 0$$

which implies $x = l(\bar{\theta} + a\sin(\sigma))$. Substituting for x in Eq. (2.15), the reduced system will be obtained as

$$\frac{d\bar{\theta}_r}{d\sigma} = \delta Q(\bar{\theta}_r + a\sin(\sigma))\sin(\sigma), \tag{2.16}$$

where the subscript r denotes the reduced system.

An averaging method can be used to further understand the dynamic behavior of reduced system (2.16). The averaged system can be written as

$$\frac{d\bar{\theta}_r^a}{d\sigma} = \delta\mu(\bar{\theta}_r^a) \tag{2.17}$$

$$\mu(\bar{\theta}_r^a) = \frac{1}{2\pi}\int_o^{2\pi} Q(\bar{\theta}_r^a + a\sin(\sigma))\sin(\sigma)d\sigma. \tag{2.18}$$

It is possible to find an approximation for $\mu(\bar{\theta}_r^a)$ using the Taylor series expansion for $Q(\bar{\theta}_r^a + a\sin(\sigma))$, as the following:

$$Q(\bar{\theta}_r^a + a\sin(\tau)) = Q(\bar{\theta}_r^a) + aQ'(\bar{\theta}_r^a)\sin(\sigma) + O(a^2). \tag{2.19}$$

Substituting (2.19) for $\mu(\bar{\theta}_r^a)$ in (2.18) and neglecting the higher order terms results in

$$\mu(\bar{\theta}_r^a) = \frac{a}{2}Q'(\bar{\theta}_r^a). \tag{2.20}$$

Consequently, the equation (2.17) can be expressed as

$$\frac{d\bar{\theta}_r^a}{d\sigma} = \frac{1}{2}\delta aQ'(\bar{\theta}_r^a), \tag{2.21}$$

which is the continuous version of the steepest descent method. The above deductions show that the averaged dynamics for the reduced variable $\bar{\theta}_r$ reaches the optimal value. Later deductions correspond between the reduced system and the actual system.

2.3.4 Time Scale in Extremum Seeking Control

The structure of an extremum seeking control method is built upon the separation of time scales in the control loop. It is very important to understand time scales exist in the overall dynamic behavior of an ESC loop. In a typical extremum seeking strategy, three separate time scales exist that can be expressed by (Tan et al. 2010):

1. **Fast time variations:** the internal dynamics of x state asymptotically regulate to $l(\theta)$.

2. **Intermediate time variations:** the dither signal $a\sin(\omega t)$ perturbs the searching state θ to explore the mapping in a small neighborhood of $\bar{\theta}$.

3. **Slow time variations:** The adaptation of the averaged state $\bar{\theta}$ to gradually converge to the optimal value.

The behavior of an ESC loop can be understood according to the existing separate time scales.

Chapter 3

RISE Extremum Seeking Control for Systems with Time-Varying Optimal Point

3.1 Motivation and Problem Statement

Most of the extremum seeking control methods in the literature consider time-invariant input-to-output mappings. In Chapter 2, the time scales in a typical ESC process were discussed. The mapping dynamic is the fastest. The perturbation has intermediate dynamics while the adaptation is the slowest. If the mapping and consequently, the extremum, are time-varying, there is a limitation for the current extremum seeking methods to work properly. It is essential that the time variations of the mapping are much slower than the adaptation dynamics (Tan et al. 2010). Krstic 2000 proposed an extremum seeking algorithm for time varying mappings. However, the structure of the variation should be known. An open problem persists in case where the input-to-output mapping is time varying with a general form and with no strong assumptions on the variation structures.

Aside from its academic importance, generalizing the ESC results to time-varying mappings might be useful in many practical applications. For example, in a wind turbine the variations of the power map are considerable and also very difficult to model. Therefore, a successful maximum power point tracking method should have the capability to identify and track the time-varying optimal operating points. It is conceivable that an ESC algo-

rithm which assumes time-invariant mappings might not perform properly if applied to this problem.

3.1.1 Extremum Seeking for Time Dependent Mappings

Numerous optimization problems seek the optimal value of θ where $Q(\theta^*) = Q^*$ is the maximum value of Q. A possible extension can be described as follows. Consider the case where the cost function is not only a function of θ, but also a function of another variable $\varrho = \varrho(t) \in \mathbb{R}$, i.e., $Q = Q(\theta, \varrho)$. In this case, the optimal value of Q depends on the value of ϱ, i.e. $\theta^* = \theta^*(\varrho)$. The optimization problem would be to find the optimal value of Q at each time. The extremum seeking problem is stated in the following.

Problem 1. *Consider a time dependent mapping $Q(\theta, \varrho(t)) : \mathbb{R} \times \mathbb{R} \to \mathbb{R}$. The optimal variable $\theta^*(t)$ is defined so that*

$$Q(\theta^*(t), \varrho(t)) > Q(\theta, \varrho(t)), \ \theta \neq \theta^*(t). \tag{3.1}$$

We denote the optimal value by $Q^*(t) \triangleq Q(\theta^*(t), \varrho(t))$. The mapping $Q(\theta, \varrho)$, the optimal variable $\theta^*(t)$, the optimal value $Q^*(t)$, and the signal $\varrho(t)$ are all unknown. Design an extremum seeking control loop such that the variable θ very nearly reaches the optimal value $\theta^*(t)$. The measurements of $\theta(t)$ and $y(t) = Q(\theta, \varrho(t))$ are available.

In this thesis, an extremum seeking control similar to the classic extremum seeking architecture is proposed. Specifically, a sinusoidal perturbation is applied to excite the searching variable $\bar{\theta}(t)$ to estimate the gradient. Afterwards, a gradient search is developed for robust tracking of the optimal point. The structure of the control loop is shown in Figure. 3.1. As can be seen, there are two components, namely, gradient search and gradient estimation, in the loop which should be appropriately designed.

3.1.2 Gradient Search for Tracking a Time Varying Optimal Point

In classic extremum seeking control methods, an effective update law for the variable $\bar{\theta}$ is the continuous steepest descent method. This update law results in asymptotic convergence to

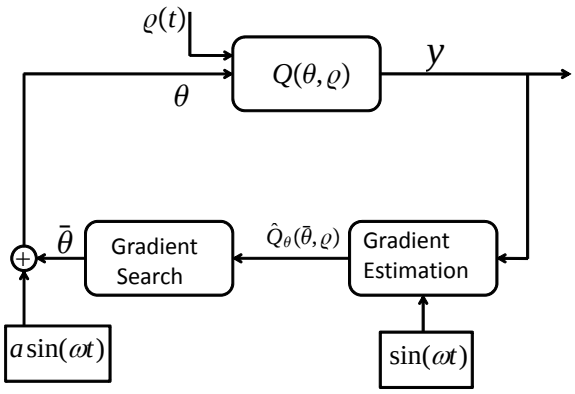

Figure 3.1: *Schemactic of extremum seeking control loop for mappings with time-varying optimal point.*

a constant optimal point. However, in the case of time-varying optimal point, only bounded error can be obtained. In this thesis, we are looking for alternative gradient search methods which can guarantee asymptotic convergence to a time-varying optimal point.

Problem 2. *Consider an update law for* $\bar{\theta}$ *of the form*

$$\dot{\bar{\theta}} = \mathcal{F}(t). \tag{3.2}$$

Design $\mathcal{F}(t)$ *such that*

$$\left|\bar{\theta} - \theta^*(t)\right| \to 0 \text{ as } t \to \infty. \tag{3.3}$$

The measurements of $\bar{\theta}(t)$ *and* $Q_\theta(\bar{\theta}, \varrho)$ *are available for feedback.*

There are several challenges associated with this problem. For example, since the optimal point $\theta^*(t)$ is completely unknown, no feed-forward term is available to be used in the control law for asymptotic tracking of the optimal point. One possible approach is to consider the variations of $\theta^*(t)$ as unstructured uncertainties and to use the ideas of robust tracking techniques.

3.1.3 Real-time Gradient Estimation

In classic extremum seeking methods, the gradient of the cost function emerges in the averaged system. However, the gradient search method in this section requires the gradient *directly*, a necessity discussed later. Therefore, we are interested in a strategy to extract the gradient signal at any given point in time.

Problem 3. *A sinusoidal perturbation is added to* $\bar{\theta}$. *The measurements of* $y = Q(\bar{\theta} + a\sin\omega t, \varrho)$ *are available. Design a strategy to extract* $Q_\theta(\bar{\theta}, \varrho)$ *at any given point in time.*

The proposed strategy in this chapter is implemented through the introduction of a delayed signal.

3.1.4 Chapter Overview

In this chapter, the method of sinusoidal perturbation is first utilized to extract the gradient in Section 3.2. In Section 3.3, a robust gradient search technique is proposed so that the trajectory of the optimal point can be asymptotically tracked using the gradient information. Afterwards, the gradient estimator and the gradient search method are combined to establish an extremum seeking control algorithm in Section 3.4. The proposed extremum seeking method has the ability to seek the optimal values of a static mapping where both the optimal point and the optimal value of the cost function are allowed to evolve over time.

3.2 Delay-Based Dynamic Estimation of Gradient Vector

In this section, a strategy for estimation of the gradient Q_θ is provided. The gradient estimation strategy is realized by adding a sinusoidal perturbation and introducing a delayed signal. The main focus in this section is to quantify the estimation error. Particularly, it is of interest to see how the time variations of the mapping Q will affect the estimation accuracy.

Lemma 3.1. *For $T = \dfrac{2\pi}{\omega}$, the following equality is valid*

$$\frac{1}{2\pi}\int_{t-T}^{t} \sin(\omega\tau + \psi)\sin(\omega\tau + \varphi)d\tau = \frac{1}{2\omega}\cos(\psi - \varphi). \tag{3.4}$$

Lemma 3.2. *Assume that the time derivative of a given function $g(t)$ is bounded, i.e.,*

$$|\dot{g}| \leq U_{\dot{g}}, \tag{3.5}$$

where $U_{\dot{g}} \in \mathbb{R}^{\geq 0}$ is a non-negative constant. Define the signal $z(t)$ as

$$z(t) = g(t)\sin(\omega t). \tag{3.6}$$

Generate the signal $z_h(t)$ by high-pass-filtering the signal $z(t)$, i.e.,

$$z_h(t) = \frac{s}{s + \omega_h} g(t)\sin(\omega t). \tag{3.7}$$

Define an error function

$$e_h = z_h(t) - g(t)w_h(t), \tag{3.8}$$

where $w_h(t)$ is generated as

$$w_h = \frac{s}{s + \omega_h}\sin(\omega t). \tag{3.9}$$

Neglecting the transient period, the error function $e_h(t)$ can be bounded as

$$|e_h| \leq U_{\dot{g}}\frac{1}{\sqrt{\omega^2 + \omega_h^2}}. \tag{3.10}$$

Proof. Define $z_l(t)$ and $w_l(t)$ respectively as

$$z_l(t) \triangleq z(t) - z_h(t), \tag{3.11}$$

$$w_l(t) \triangleq \sin(\omega t) - w_h(t). \tag{3.12}$$

According to the above definitions, (3.7), and (3.9),

$$z_l(t) = \frac{\omega_h}{s + \omega_h} g(t)\sin(\omega t), \tag{3.13}$$

$$w_l(t) = \frac{\omega_h}{s + \omega_h}\sin(\omega t). \tag{3.14}$$

From (3.14), it can be concluded that

$$|w_l(t)| \leq \frac{\omega_h}{\sqrt{\omega^2 + \omega_h^2}}. \tag{3.15}$$

According to the definition of $e_h(t)$ in (3.8),

$$\begin{aligned} e_h(t) &= z_h(t) - g(t)w_h(t) \\ &= (z(t) - z_l(t)) - g(t)\left(\sin(\omega t) - w_l(t)\right) \\ &= (g(t)w_l(t) - z_l(t)) + (z(t) - g(t)\sin(\omega t)) \\ &= g(t)w_l(t) - z_l(t). \end{aligned} \tag{3.16}$$

From (3.13) and (3.14),

$$\dot{z}_l(t) = -\omega_h z_l(t) + \omega_h g(t)\sin(\omega t), \tag{3.17}$$

$$\dot{w}_l(t) = -\omega_h w_l(t) + \omega_h \sin(\omega t). \tag{3.18}$$

Taking the derivative of e_h and using (3.17) and (3.18),

$$\begin{aligned} \dot{e}_h(t) &= \dot{g}(t)w_l(t) + g(t)\dot{w}_l(t) - \dot{z}_l(t) \\ &= \dot{g}(t)w_l(t) + g(t)\left\{-\omega_h w_l(t) + \omega_h \sin(\omega t)\right\} \\ &\quad - \left\{-\omega_h z_l(t) + \omega_h g(t)\sin(\omega t)\right\} \\ &= \dot{g}(t)w_l(t) - \omega_h\left\{g(t)w_l(t) - z_l(t)\right\} \\ &\quad + \left\{g(t)\omega_h \sin(\omega t) - \omega_h g(t)\sin(\omega t)\right\} \\ &= \dot{g}(t)w_l(t) - \omega_h e_h. \end{aligned} \tag{3.19}$$

Based on (3.19), $e_h(t)$ can be rewritten as

$$e_h(t) = \frac{1}{s + \omega_h}\dot{g}(t)w_l(t). \tag{3.20}$$

Therefore, $|e_h|$ can be bounded as

$$|e_h| \leq \frac{1}{\omega_h} U_{\dot{g}} \frac{\omega_h}{\sqrt{\omega^2 + \omega_h^2}} = U_{\dot{g}} \frac{1}{\sqrt{\omega^2 + \omega_h^2}}, \tag{3.21}$$

according to (3.20), (3.5), and (3.15). □

Remark 2. *Lemma 3.2 will be used in subsequent analysis to quantify the error induced by variations in the mapping. According to Lemma 3.2, if the time-variation of function $g(t)$ is small, a good estimate for $z_h(t)$ defined in (3.7) can be given as $g(t)w_h(t)$, where $w_h(t)$ is defined in (3.9).*

Definition 1. *A system is constructed as follows:*

1. *The signals $\bar{\theta}(t) \in \mathbb{R}$ and $\varrho(t) \in \mathbb{R}$ are functions of time with bounded variation rates, i.e.,*
$$|\dot{\bar{\theta}}(t)| + |\dot{\varrho}(t)| \leq \varepsilon. \tag{3.22}$$

2. *A sinusoidal dither signal with perturbation amplitude a and the frequency ω is added to the signal $\bar{\theta}(t)$ to generate $\theta(t)$, i.e.,*
$$\theta(t) = \bar{\theta}(t) + a\sin(\omega t). \tag{3.23}$$

3. *The signal $y(t) = Q(\theta(t), \varrho(t)$ is generated by a smooth function $Q(\theta, \varrho) : \mathbb{R} \times \mathbb{R} \to \mathbb{R}$ and its measurements are available at any given point in time.*

4. *The signal $y(t)$ is passed through a high-pass filter $\dfrac{s}{s+\omega_h}$ to generate the signal $Q_h(\theta(t), \varrho(t))$, i.e.,*
$$Q_h(\theta, \varrho) \triangleq \frac{s}{s+\omega_h} Q(\theta, \varrho). \tag{3.24}$$

5. *The signal $\mu(\theta(t), \varrho(t))$ is generated as*
$$\mu(\theta(t), \varrho(t)) \triangleq \frac{1}{2\pi} \frac{1 - e^{-Ts}}{s} \left\{ Q_h(\theta, \varrho) \sin(\omega\tau + \varphi) \right\}, \tag{3.25}$$
where $T = \dfrac{2\pi}{\omega}$ and $\varphi \in [0, 2\pi)$ is the demodulation phase angle.

To facilitate the subsequent analysis, following assumptions are made.

Assumption 1. *The perturbation amplitude a is small.*

Assumption 2. *The values of $Q_{\theta\theta}(\bar{\theta}(t), \varrho(t))$ and $Q_{\varrho\theta}(\bar{\theta}(t), \varrho(t))$ remain bounded.*

Assumption 3. *The variations of $\bar{\theta}(t)$ and $\varrho(t)$ satisfy*

$$\int_{t-T}^{t} Q_h(\bar{\theta}, \varrho)\sin(\omega t + \varphi)d\tau \cong 0, \tag{3.26}$$

where $Q_h(\bar{\theta}, \varrho)$ is generated by high-pass-filtering of the signal $Q(\bar{\theta}, \varrho)$.

Remark 3. *Assumptions 1 is a common assumption for developing an extremum seeking algorithm (Ariyur and Krstic 2003). Assumption 2 will be used in the subsequent analysis. Assumption 3 indicates that the variations of $Q_h(\bar{\theta}, \varrho)$ with the frequency ω are negligible.*

Theorem 3.3. *Consider the system constructed in Definition 1. Assume that Assumptions 1-3 hold. The signal $\mu(\theta, \varrho)$, defined in (3.25), can be determined as*

$$\mu(\bar{\theta}, \varrho) = \frac{1}{2\omega} af\cos(\varphi - \psi)Q_\theta(\bar{\theta}, \varrho) + \epsilon_{est}(\cdot), \tag{3.27}$$

where f and ψ are the magnitude scale and angle shift caused by the high-pass frequency filter and the estimation error $\epsilon_{est}(\cdot)$ is

$$\epsilon_{est}(\cdot) = \mathcal{O}(\frac{\varepsilon a}{\omega^2} + \frac{a^2}{\omega}). \tag{3.28}$$

Proof. Using the Taylor expansion for multi-variable functions, $Q(\theta, \varrho)$ can be expanded at $(\bar{\theta}, \varrho)$ as

$$Q(\theta, \varrho) = \sum_{i=0}^{\infty} (\delta_\theta \frac{\partial}{\partial \theta})^i Q\Big|_{(\bar{\theta}, \varrho)}, \tag{3.29}$$

where according to (3.23), $\delta_\theta \triangleq a\sin(\omega t)$. By substituting for δ_θ in (3.29), we get

$$Q(\theta, \varrho) = Q(\bar{\theta}, \varrho) + aQ_\theta(\bar{\theta}, \varrho)\sin(\omega t) + \epsilon_1(\cdot), \tag{3.30}$$

where

$$\epsilon_1(\cdot) = a^2 Q_{\theta\theta}(\bar{\theta}, \varrho)\sin^2(\omega t) + ... = \mathcal{O}(a^2). \tag{3.31}$$

According to the system description and Assumption 2, the time derivative of $Q_\theta(\bar{\theta}, \varrho)$ in (3.30) will be bounded. Hence, the following inequality is true

$$\left|\frac{d}{dt} Q_\theta(\bar{\theta}, \varrho)\right| \leq C\varepsilon, \tag{3.32}$$

where C is a positive constant.

The filtered signal $Q_h(\theta, \varrho)$ can be approximated by

$$Q_h(\theta, \varrho) = Q_h(\bar{\theta}, \varrho) + afQ_\theta(\bar{\theta}, \varrho)\sin(\omega t + \psi) + \epsilon_2(\cdot), \tag{3.33}$$

where

$$\epsilon_2(\cdot) \triangleq \mathcal{O}(a^2, a\varepsilon\frac{1}{\sqrt{\omega^2 + \omega_h^2}}) \tag{3.34}$$

according to Eq. (3.31) and Lemma 3.2.

It is easy to show that

$$\begin{aligned}
\mu(\theta, \varrho) &= \frac{1}{2\pi}\frac{1 - e^{-Ts}}{s}\{Q_h(\theta, \varrho)\sin(\omega\tau + \varphi)\} \\
&= \frac{1}{2\pi}\int_{t-T}^{t} Q_h(\theta, \varrho)\sin(\omega\tau + \varphi)d\tau \\
&= \mu(\bar{\theta}, \varrho) + \frac{1}{2\pi}\int_{t-T}^{t} afQ_\theta(\bar{\theta}, \varrho) \\
&\quad \sin(\omega\tau + \psi)\sin(\omega\tau + \varphi)d\tau + \epsilon_3(\cdot),
\end{aligned} \tag{3.35}$$

where

$$\begin{aligned}
\epsilon_3(\cdot) &\triangleq \frac{1}{2\pi}\int_{t-T}^{t} \epsilon_2(\cdot)\sin(\omega\tau + \varphi)d\tau \\
&= \mathcal{O}(\frac{a^2}{\omega}, a\varepsilon\frac{1}{\omega\sqrt{\omega^2 + \omega_h^2}}).
\end{aligned} \tag{3.36}$$

Using the relations in Lemma 3.1, it can be shown that (see Appendix for the proof)

$$\begin{aligned}
&\frac{1}{2\pi}\int_{t-T}^{t} afQ_\theta(\bar{\theta}, \varrho)\sin(\omega\tau + \psi)\sin(\omega\tau + \varphi)d\tau \\
&\quad = \frac{1}{2\omega}af\cos(\varphi - \psi)Q_\theta(\bar{\theta}(t), \varrho(t)) + \epsilon_4(\cdot),
\end{aligned} \tag{3.37}$$

where

$$\epsilon_4(\cdot) \triangleq \mathcal{O}(a\varepsilon\frac{1}{\omega^2}). \tag{3.38}$$

Based on Assumption 3, $\mu(\bar{\theta}, \varrho)$ is negligible. Therefore, $\mu(\theta, \varrho)$ can be expressed as

$$\mu(\theta, \varrho) = \frac{1}{2\omega}af\cos(\varphi - \psi)Q_\theta(\bar{\theta}(t), \varrho(t)) + \epsilon_{est}(\cdot), \tag{3.39}$$

where

$$\begin{aligned}\epsilon_{est}(\cdot) &\triangleq \epsilon_4(\cdot)+\epsilon_3(\cdot)\\ &= \mathcal{O}(\frac{a^2}{\omega}, a\varepsilon\frac{1}{\omega\sqrt{\omega^2+\omega_h^2}}, a\varepsilon\frac{1}{\omega^2})\\ &= \mathcal{O}(\frac{\varepsilon a}{\omega^2}+\frac{a^2}{\omega}).\end{aligned} \tag{3.40}$$

□

In this paper, we use the first order high-pass filter of the form

$$HPF(s)=\frac{s}{s+\omega_h}. \tag{3.41}$$

in the control loop. In addition we select the demodulation phase angle $\varphi=0$. By such choices, the values computed for f and ψ are obtained as

$$f=\frac{\omega}{\sqrt{\omega^2+\omega_h^2}},\quad \psi=\frac{\pi}{2}-\tan^{-1}(\frac{\omega}{\omega_h}). \tag{3.42}$$

Furthermore, the $\cos(\varphi-\psi)$ term in (3.39) can be calculated as

$$\begin{aligned}\cos(\varphi-\psi) &= \cos(\psi)=\cos(\frac{\pi}{2}-\tan^{-1}(\frac{\omega}{\omega_h}))\\ &= \sin(\tan^{-1}(\frac{\omega}{\omega_h}))=\frac{\omega}{\sqrt{\omega^2+\omega_h^2}}.\end{aligned} \tag{3.43}$$

Therefore, neglecting the higher order error terms in (3.39), $\mu(\theta,\varrho)$ can be expressed as follows

$$\mu(\theta,\varrho)\simeq\frac{1}{2}\frac{a\omega}{\omega^2+\omega_h^2}Q_\theta(\bar{\theta},\varrho). \tag{3.44}$$

Note that according to the statements in Theorem 3.3, it is feasible to generate the signal $\mu(\theta,\varrho)$. In the future developments and simulations, the signal $\mu(\theta,\varrho)$ is generated for estimating the gradient $Q_\theta(\bar{\theta},\varrho)$ according to Eq. (3.44).

Example 3.1. *Select the function $Q(\theta,\varrho)$ as*

$$Q=4\varrho(t)^3-\varrho(t)(\theta(t)^2-\varrho(t))^2.$$

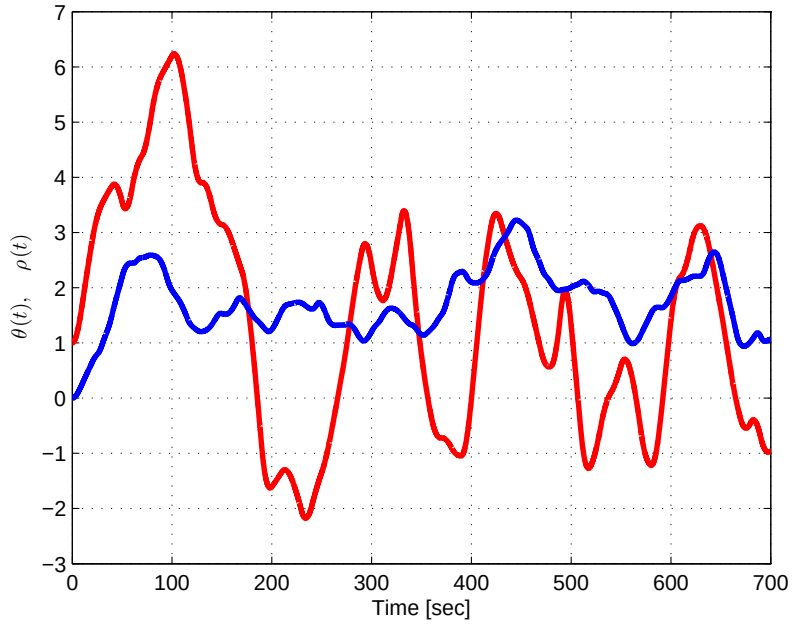

Figure 3.2: *System signals $\bar{\theta}(t)$ (blue) and $\varrho(t)$ (red) in Example 3.1.*

According to this function, an expression can be derived for the gradient of Q_θ as

$$Q_\theta = -4\varrho(t)\theta(t)(\theta^2(t) - \varrho(t)).$$

The signals $\bar{\theta}$ and ϱ are generated through low pass filtering random pulses and are shown in Fig.3.2. A perturbation with the frequency $\omega = 3$ with the amplitude $a = 0.1$ is added to the signal $\bar{\theta}$. The high-pass-filter frequency is selected as $\omega_h = 2$. The gradient estimation algorithm in Theorem 3.3 is employed to estimate the gradient. The real and estimated gradient signals are shown in Fig.3.3.

3.3 RISE Gradient Search

3.3.1 Problem Formulation

If $\theta^*(t) = \theta^*$ is constant through time, it can be shown that the update law

$$\mathcal{F}(t) = \alpha Q_\theta, \tag{3.45}$$

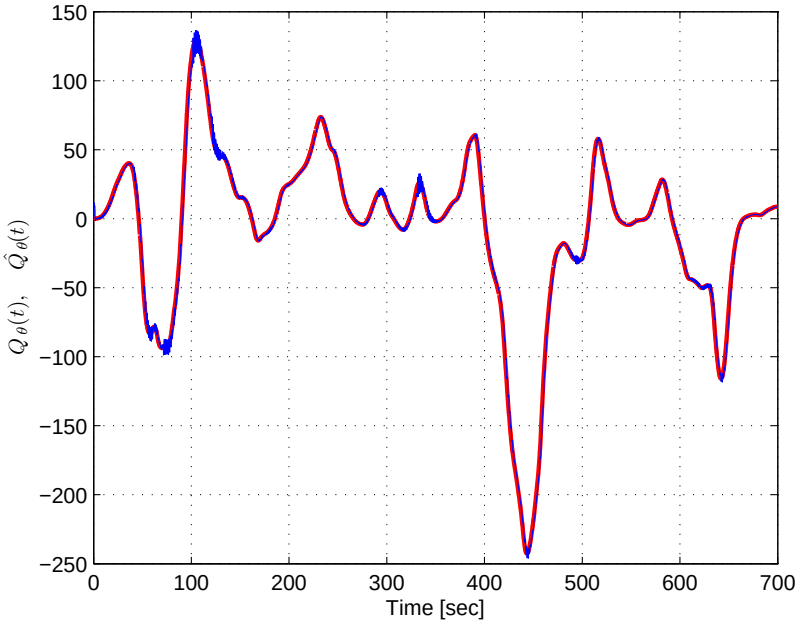

Figure 3.3: *Actual (red) and estimated (blue) gradient in Example 3.1.*

with α being a positive scalar, will make $\bar{\theta}$ asymptotically converge to the optimal point. The asymptotic tracking for general time varying case is much more challenging. If θ^* is a function of time, the update law (3.45) will result in bounded tracking error.

Prior to proceeding to the next theorem which proposes the control law for solving the time-varying case, assume the following.

Assumption 4. *The first partial derivative Q_θ exists and at the optimal point, θ^* is equal to zero. The second partial derivative $Q_{\theta\theta}$ exists at the optimal point θ^* and is negative. Furthermore,*

$$Q_\theta(\theta^* + \xi, \varrho(t))\xi < 0 \text{ for every } \xi \neq 0, \tag{3.46}$$

where $\xi \in \mathbb{R}$ is defined as

$$\xi \triangleq \bar{\theta} - \theta^*. \tag{3.47}$$

Remark 4. *Condition (3.46) implies that there is only a single maximum and the gradient is zero only at the maximum point. Having the second partial derivative $Q^*_{\theta\theta}$ negative is a*

sufficient condition, but not a necessary condition, for having maximum. However, since in the future analysis the optimum is searched only using the gradient, having $Q^*_{\theta\theta}$ negative is required to guarantee asymptotic convergence to the extremum.

Since $Q^*_{\theta\theta}$ exists and is negative, the function $\gamma^*(\varrho)$ defined as

$$\gamma^*(\varrho) = -\lim_{\xi \to 0} \frac{Q_\theta(\theta^* + \xi, \varrho)}{\xi} = -Q^*_{\theta\theta}, \tag{3.48}$$

exists and is always positive. Furthermore, the function $\gamma(\xi, \varrho)$ defined as

$$\gamma(\xi, \varrho) = \begin{cases} -\dfrac{Q_\theta(\theta^* + \xi, \varrho)}{\xi}, & \xi \neq 0 \\ \gamma^*(\varrho), & \xi = 0 \end{cases} \tag{3.49}$$

also exists and is positive.

Based on the definition (3.47),

$$\dot{\xi} = \mathcal{F}(t) - \dot{\theta}^*(t). \tag{3.50}$$

According to (3.50) and the definition of ξ in (3.47), the optimization problem can be reduced to a robust stabilization problem for the system in (3.50). Here, the term $\dot{\theta}^*(t)$ should be considered as an uncertain disturbance. A successful method for solving robust stabilization with uncertain disturbances was developed in Makkar et al. Oct. 2007, Xian et al. July 2004. Since Patre et al. 2008, this control strategy is termed as Robust Integral of the Sign of the Error (RISE). The RISE control method has the significant ability to enable asymptotic stability in the presence of sufficiently smooth disturbances. In this section, a relevant method to design a robust gradient search method is used. The following assumptions allows for application of a RISE strategy to the gradient search problem.

Assumption 5. *The function $\gamma(\xi, \varrho)$ is strictly greater than a positive value, i.e., $\gamma \geq \gamma_0 > 0$, in a bounded interval I containing the origin. Furthermore, the partial derivatives γ_ξ and γ_ϱ are bounded.*

Remark 5. *The term $\gamma(\xi, \varrho)$ is always positive. In a bounded interval I, $\gamma(\xi, \varrho)$ has a minimum greater than zero. Therefore, the above assumption is reasonable. Boundedness of γ_ξ and γ_ϱ are used in the future analysis.*

Assumption 6. *The first three derivatives of θ^* are bounded, i.e., $\dot{\theta}^*, \ddot{\theta}^*, \dddot{\theta}^* \in \mathcal{L}_\infty$. We denote the upper bounds by $U_{\dot{\theta}^*}, U_{\ddot{\theta}^*}$, and $U_{\dddot{\theta}^*}$, respectively. In addition, $\dot{\varrho}$ is also bounded, i.e., $\dot{\varrho} \in \mathcal{L}_\infty$.*

Remark 6. *In this section, we are looking for a gradient search which can asymptotically track the extremum. The smoothness of θ^* is a key point in the subsequent analysis.*

The following controller is designed for the gradient search problem introduced in Section 3.3.1,

$$\mathcal{F}(t) = k_1 Q_\theta + \Phi - c_1 \bar{\theta} \tag{3.51}$$

$$\dot{\Phi} = c_2 k_1 Q_\theta + k_2 sgn(Q_\theta), \tag{3.52}$$

where c_1, c_2, k_1, k_2 are positive design gains to be determined later.

In the following section, the error system is developed and then the stability analysis is provided.

3.3.2 Error System Development

According to the definition of $\gamma(\xi, \varrho)$ in (3.49), the following is true

$$Q_\theta = -\gamma(\xi, \varrho)\xi. \tag{3.53}$$

In the subsequent analysis, the positiveness of $\gamma(\xi, \varrho)$ is used. The term in (3.52) can be expressed as

$$sgn(Q_\theta) = sgn(-\gamma\xi) = -sgn(\xi), \tag{3.54}$$

for $\gamma(\xi, \varrho)$ is positive. Using (3.53) and (3.54), the controller (3.51) can be rewritten as

$$\mathcal{F}(t) = -k_1 \gamma \xi + \Phi - c_1 \bar{\theta}, \tag{3.55}$$

$$\dot{\Phi} = -c_2 k_1 \gamma \xi - k_2 sgn(\xi). \tag{3.56}$$

Define a filtered signal $\eta \in \mathbb{R}$ as

$$\eta \triangleq \dot{\xi} + c_2 \xi, \tag{3.57}$$

where $c_2 \in \mathbb{R}^{>0}$ is a positive constant. The derivative of η can be obtained using (3.55-3.57) as

$$\begin{aligned}
\dot{\eta} &= -k_1\dot{\gamma}\xi - k_1\gamma\dot{\xi} - c_2k_1\gamma\xi - k_2 sgn(\xi) \\
&\quad -c_1\dot{\bar{\theta}} - \ddot{\theta}^* + c_1\dot{\xi} + (c_2 - c_1)\dot{\xi} \\
&= -k_1(\gamma_\xi(\eta - c_2\xi) + \gamma_\varrho\dot{\varrho})\xi - k_1\gamma\eta - k_2 sgn(\xi) \\
&\quad -c_1\dot{\theta}^* - \ddot{\theta}^* + (c_2 - c_1)(\eta - c\xi) \\
&= -k_1\gamma\eta - k_2 sgn(\xi) + N_c(t) + \tilde{N}(t) \qquad (3.58)
\end{aligned}$$

where the last two terms are

$$\begin{aligned}
\tilde{N}(t) &= -k_1\gamma_\xi\eta\xi + c_2k_1\gamma_\xi\xi^2 \\
&\quad -k_1\gamma_\varrho\dot{\varrho}\xi + (c_2 - c_1)(\eta - c_2\xi), \qquad (3.59) \\
N_c(t) &= -\ddot{\theta}^* - c_1\dot{\theta}^*. \qquad (3.60)
\end{aligned}$$

Based on the definition of $N_c(t)$ in (3.60) and Assumption 6, $N_c(t)$ can be bounded as

$$|N_c(t)| \leq U_{\ddot{\theta}^*} + c_1U_{\dot{\theta}^*} \leq U_{N_c}. \qquad (3.61)$$

Similarly, $\dot{N}_c(t)$ obtained as

$$\dot{N}_c(t) = -\dddot{\theta}^* - c_1\ddot{\theta}^*, \qquad (3.62)$$

is bounded by

$$\left|\dot{N}_c(t)\right| \leq U_{\dddot{\theta}^*} + c_1U_{\ddot{\theta}^*} \leq U_{\dot{N}_c}. \qquad (3.63)$$

Based on (3.59) and the boundedness of γ_ξ, γ_ϱ, and $\dot{\varrho}$, $\left|\tilde{N}(t)\right|$ can be bounded as

$$\left|\tilde{N}(t)\right| \leq \rho(\|\chi\|)\,\|\chi\|\,, \qquad (3.64)$$

where $\rho(\|\chi\|)$ is an invertible positive non-decreasing function and χ is defined as

$$\chi \triangleq [\xi\ \eta]^T. \qquad (3.65)$$

3.3.3 Stability Analysis

Theorem 3.4. *Consider the gradient search problem described in Section 3.3.1. Suppose that Assumptions 4-6 hold. The controller (3.51) makes $\bar{\theta}$ in the system (3.2) asymptotically track the optimal value $\theta^*(t)$, provided that the control gains c_1, c_2, k_1, k_2 are designed so that*

$$c_2 > \frac{1}{2}, \;\; k_2 > U_{N_c} + \frac{1}{c_2} U_{\dot{N}_c} \tag{3.66}$$

and k_1 is sufficiently large.

Proof. Let $\mathcal{D} \subset \mathbb{R}^4$ be a domain containing $\mathcal{Y}(t) = 0$, where $\mathcal{Y}(t) \in \mathbb{R}^3$ is defined as $\mathcal{Y}(t) \triangleq [\chi^T(t), \sqrt{W(t)}]^T$ where $\chi(t) = [\xi \;\; \eta]^T$, and the auxiliary function $W(t) \in \mathbb{R}$ is defined as

$$W(t) \triangleq k_2 \left|\xi(0)\right| - \xi(0) N_c(0) - \int_0^t L(\tau) d\tau, \tag{3.67}$$

where $k_2 \in \mathbb{R}$ is nonnegative by design. In (3.67), the auxiliary function $L(t) \in \mathbb{R}$ is defined as

$$L(t) \triangleq \eta (N_c(t) + k_2 sgn(Q_\theta)). \tag{3.68}$$

Since $sgn(Q_\theta) = -sgn(\xi)$, the time derivative of $W(t)$ can be written as

$$\dot{W}(t) = -L(t) = -\eta (N_c(t) - k_2 sgn(\xi)). \tag{3.69}$$

Provided that

$$k_2 > U_{N_c} + \frac{1}{c_2} U_{\dot{N}_c}, \tag{3.70}$$

the following inequality can be obtained (see Xian et al. July 2004 for the proof):

$$\int_0^t L(\tau) d\tau \leq k_2 \left|\xi(0)\right| - \xi(0) N_c(0). \tag{3.71}$$

Hence, (3.71) can be used to conclude that $W(t) \geq 0$.

Let $V(\mathcal{Y}, t) \in \mathbb{R}$ be a continuously differentiable positive definite function defined as

$$V(\mathcal{Y}, t) \triangleq \frac{1}{2} m \xi^2 + \frac{1}{2} \eta^2 + W, \tag{3.72}$$

where $m \in \mathbb{R}^{>0}$ is a positive constant.

Function $V(\mathcal{Y}, t)$ in (3.72) can be bounded as

$$\frac{1}{2}\min\{m, 1\}\left\|\mathcal{Y}\right\|^2 \leq V(\mathcal{Y}, t) \leq \max\{\frac{m}{2}, 1\}\left\|\mathcal{Y}\right\|^2. \tag{3.73}$$

The time derivative of $V(\mathcal{Y}, t)$ is

$$\begin{aligned}
\dot{V} &= m\xi\dot{\xi} + \eta\dot{\eta} + \dot{W} \\
&= m\xi(\eta - c_2\xi) + \eta(-k_1\gamma\eta - k_2 sgn(\xi) + N_c(t) \\
&\quad + \tilde{N}(t)) - \eta(N_c(t) - k_2 sgn(\xi)) \\
&= -mc_2\xi^2 + m\xi\eta - k_1\gamma\eta^2 + \eta\tilde{N}(t)
\end{aligned} \tag{3.74}$$

by using (3.57), (3.58), and (3.69).

The term $\xi\eta$ can be upper bounded as

$$\xi\eta \leq \frac{1}{2}\left(\xi^2 + \eta^2\right). \tag{3.75}$$

Using the relations (3.64) and (3.75), Eq. (3.74) becomes

$$\begin{aligned}
\dot{V} &\leq -m(c_2 - \frac{1}{2})\xi^2 + \frac{1}{2}m\eta^2 \\
&\quad -k_1\gamma_0\eta^2 + \rho(\left\|\chi\right\|)\left\|\chi\right\|\left|\eta\right|.
\end{aligned} \tag{3.76}$$

Let us write the control gain k_1 as

$$k_1 = \frac{k_\eta}{\gamma_0} + \frac{k_\chi}{\gamma_0}, \tag{3.77}$$

to get the following relation

$$\begin{aligned}
\dot{V} &\leq -m(c_2 - \frac{1}{2})\xi^2 - (k_\eta - \frac{1}{2}m)\eta^2 \\
&\quad -k_\chi\eta^2 + \rho(\left\|\chi\right\|)\left\|\chi\right\|\left|\eta\right| \\
&\leq -m(c_2 - \frac{1}{2})\xi^2 - (k_\eta - \frac{1}{2}m)\eta^2 \\
&\quad -\left(k_\chi\left|\eta\right|^2 - \rho(\left\|\chi\right\|)\left\|\chi\right\|\left|\eta\right|\right).
\end{aligned} \tag{3.78}$$

The last term in (3.78) can be written as

$$k_\chi |\eta|^2 - \rho(\|\chi\|)\,\|\chi\|\,|\eta| = k_\chi \left(|\eta| - \frac{\rho(\|\chi\|)}{2k_\chi}\right)^2 - \frac{\rho^2(\|\chi\|)}{4k_\chi}\|\chi\|^2 . \tag{3.79}$$

Therefore, the derivative of the Lyapunov function will be

$$\begin{aligned} \dot{V} &\leq -\sigma_1 \|\chi\|^2 + \frac{\rho^2(\|\chi\|)}{4k_\chi}\|\chi\|^2 \\ &\leq -\sigma_2 \|\chi\|^2 , \end{aligned} \tag{3.80}$$

where

$$\sigma_1 = \min\{m(c_2 - \frac{1}{2}), (k_\eta - \frac{1}{2}m)\}, \tag{3.81}$$

$$\sigma_2 = \sigma_1 - \frac{\rho^2(\|\chi\|)}{4k_\chi}. \tag{3.82}$$

Selecting $c_2 > \frac{1}{2}$ and k_1 as large enough, σ_1 and σ_2 will be positive. Specifically, the function $\sigma_2 \|\chi\|^2$ is positive semi-definite on the domain

$$\mathcal{D} = \{\mathcal{Y} \in \mathbb{R}^3 \mid \|\mathcal{Y}\| \leq \rho^{-1}(2\sqrt{\sigma_1 k_\chi})\}. \tag{3.83}$$

This proves that $\|\chi\| \to 0$ as $t \to \infty$ in a subset of $\mathcal{D}$ (see Theorem 8.4 in Khalil 2002). Having $\|\chi\| \to 0$ as $t \to \infty$ indicates that $\left|\bar{\theta} - \theta^*\right| \to 0$ as $t \to 0$. □

Example 3.2. *A control law is desired to be designed so that $\bar{\theta}$ in (3.2) track the time-varying optimal point of the mapping*

$$Q = (3 + \sin(t))\left[3 - (\theta + 1 - 4\sin(t))^2\right]. \tag{3.84}$$

Only measurements of θ and $Q_\theta = -2(3 + 2\sin(t))(\bar{\theta} + 1 - \sin(t))$ are available for feedback. Based on the cost function (3.84), the optimal trajectory of $\theta(t)$ and the maximum value of Q at each time are

$$\theta^*(t) = 4\sin(t) - 1, \tag{3.85}$$

$$Q^*(t) = 3(3 + \sin(t)). \tag{3.86}$$

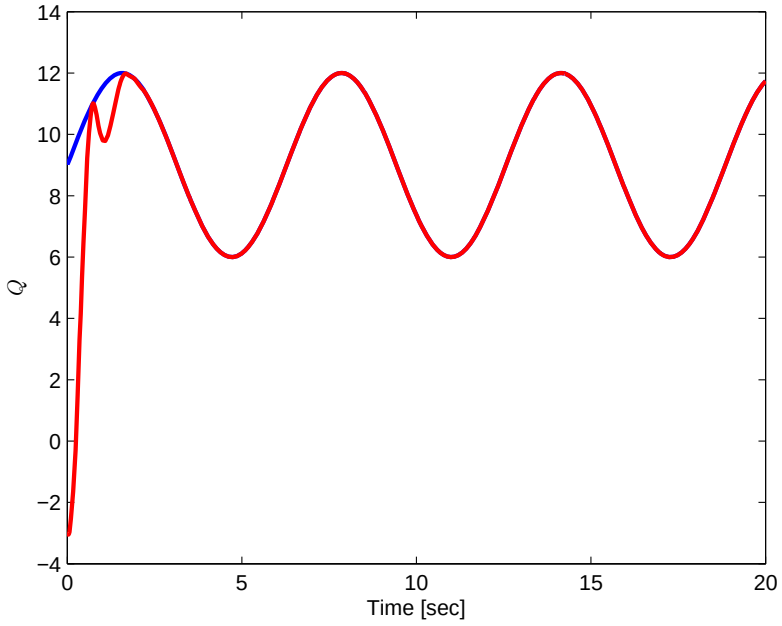

Figure 3.4: *RISE gradient search performance in Example 3.2. The obtained value of the cost function is shown in red and its maximum value $Q^*(t)$ is plotted in blue.*

As can be seen in Fig.3.4, the RISE gradient algorithm enables asymptotic tracking the optimal values. A simulation has also been performed using the algorithm (3.45) for comparison. As predicted, it can be observed in Fig.3.5 that bounded result is achieved.

3.4 RISE Extremum Seeking Control Loop

3.4.1 Extremum Seeking Loop Design

A RISE extremum seeking control is designed as follows. A perturbation is applied to the variable $\bar{\theta}$ and the delay-based gradient estimation method discussed in Section 3.2 is used to estimate the gradient. The estimated gradient is then fed into the RISE gradient search controller, designed in Section 3.3, which updates the estimates $\bar{\theta}$. A schematic of the control loop is shown in Fig.3.6.

The logic behind the control loop design relies on the assumption of the separation of

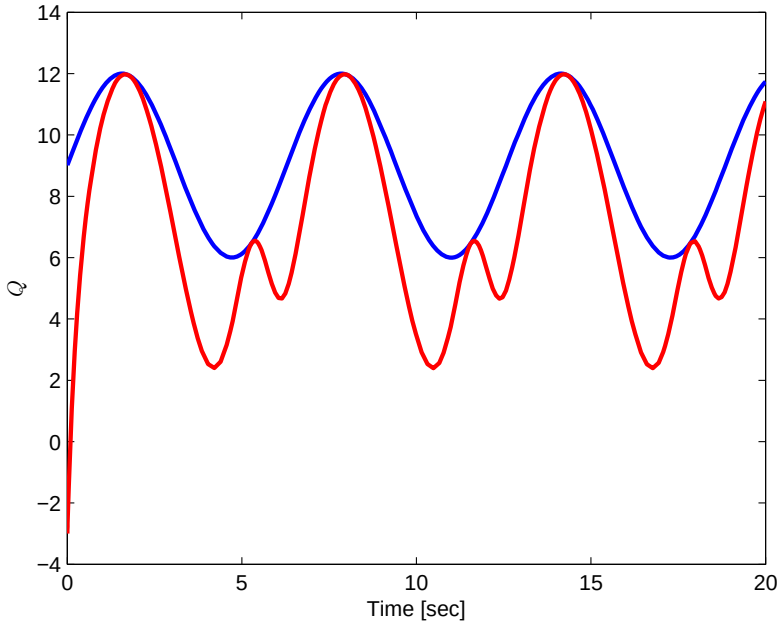

Figure 3.5: *Steepest descent gradient search performance in Example 3.2. The obtained value of the cost function is shown in red and its maximum value $Q^*(t)$ is plotted in blue.*

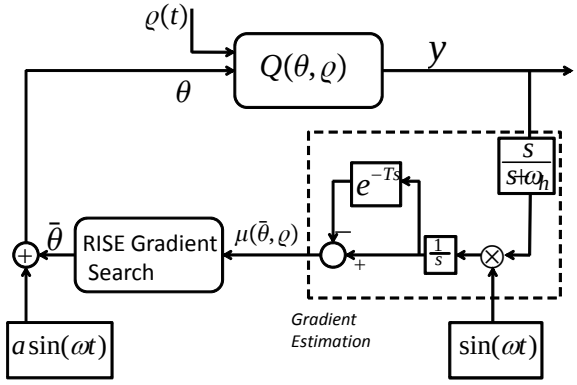

Figure 3.6: *Schematic of RISE Extremum Seeking Control Loop*

the time scales of the gradient estimation and the adaptation dynamics. Since there exists the estimation error $\epsilon_{est}(\cdot)$, specified in Eq. (3.28), between the estimated and the actual value of the gradient, the searching variable $\bar{\theta}$ will not asymptotically reach the extremum trajectory $\theta^*(t)$ but it will reach close enough if the estimation error is small.

Theorem 3.5. *Consider a mapping $Q(\theta, \varrho) : \mathbb{R} \times \mathbb{R} \to \mathbb{R}$ that satisfies Assumptions 4-5. Suppose that θ^* and ϱ satisfy Assumption 6. In the system*

$$
\begin{aligned}
y &= Q(\bar{\theta} + a\sin(\omega t), \varrho) && (3.87)\\
y_h &= \frac{s}{s+\omega_h} y && (3.88)\\
\mu &= \frac{1}{2\pi}\frac{1-e^{Ts}}{s}\{y_h \sin(\omega t)\} && (3.89)\\
e &\triangleq 2\frac{\omega^2+\omega_h^2}{a\omega}\mu && (3.90)\\
\dot{\Phi} &= c_2 k_1 e + k_2 sgn(e) && (3.91)\\
\dot{\bar{\theta}} &= k_1 e + \Phi - c_1\bar{\theta}, && (3.92)
\end{aligned}
$$

where $T = \dfrac{2\pi}{\omega}$, the signal $\bar{\theta}(t)$ closely reaches the optimal trajectory $\theta^*(t)$ if the control gains are selected properly according to Theorem 3.4, the perturbation amplitude a is small, and the perturbation frequency ω is high with respect to the variations of ϱ and $\bar{\theta}$.

Proof. If the perturbation frequency ω is high with respect to the variations of ϱ and $\bar{\theta}$ and the perturbation amplitude a is small, the gradient estimation component, which is Eq. (3.87-3.90), estimates the gradient with small error according to the error term specified in Eq. (3.28). Comparing (3.89) with (3.25) and (3.44), it is concluded that $e \simeq Q_\theta(\bar{\theta}, \varrho)$ in (3.90). Therefore, the estimated gradient is fed into the RISE gradient search according to Eq. (3.91-3.92). The gradient search moves the signal $\bar{\theta}$ towards the optimal value. However, since there is some small error in the estimated gradient, the signal $\bar{\theta}(t)$ reaches close proximity to the optimal trajectory $\theta^*(t)$. □

Example 3.3. *The proposed RISE extremum seeking control method is applied to the fol-*

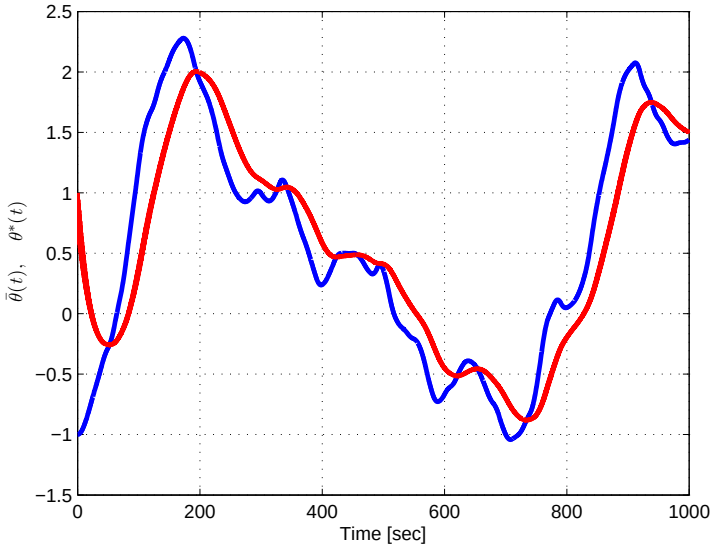

Figure 3.7: *The optimal trajectory tracking of the first order extremum seeking control method. The optimal variable $\theta^*(t)$ is shown in blue while the generated variable $\bar{\theta}(t)$ is shown in red.*

lowing static mapping

$$Q = -(\theta - \theta^* + 2)^2, \tag{3.93}$$

where the optimal trajectory $\theta^*(t)$ is arbitrarily time-varying as shown in blue in Fig.3.7. The results of the classic first-order extremum seeking method, shown in Fig. 2.3, are presented in Fig.3.7 and Fig.3.8. The control gains are selected as $a = 0.1$, $\omega = 8$, and $k = 0.2$. Simulations have been performed using the RISE extremum seeking control loop in Fig.3.6. The control constants are chosen as $a = 0.1$, $\omega = 8$, $k_1 = 0.01$, $k_2 = 0.05$, $c_1 = 0.05$, $c_2 = 0.6$. Fig.3.9 indicates that the robust ESC makes the variable track the optimal trajectory very close. Fig.3.10 shows that the cost function Q almost achieves its optimal value.

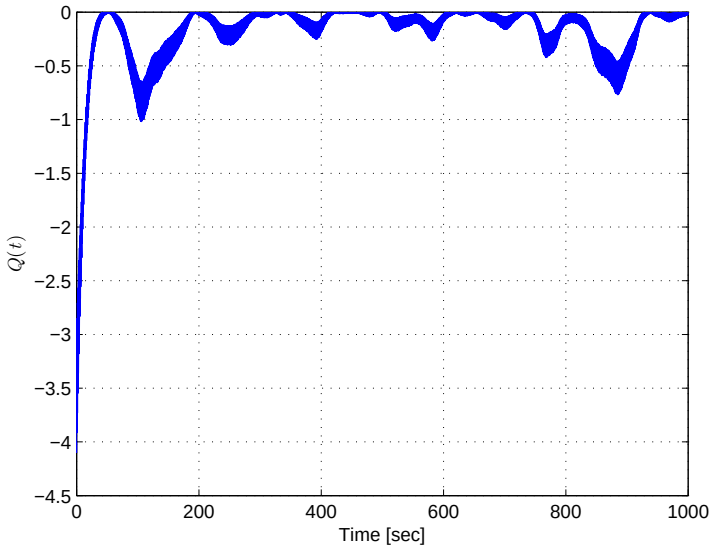

Figure 3.8: *The values of the cost function Q as a function of time, generated by the first order extremum seeking control method.*

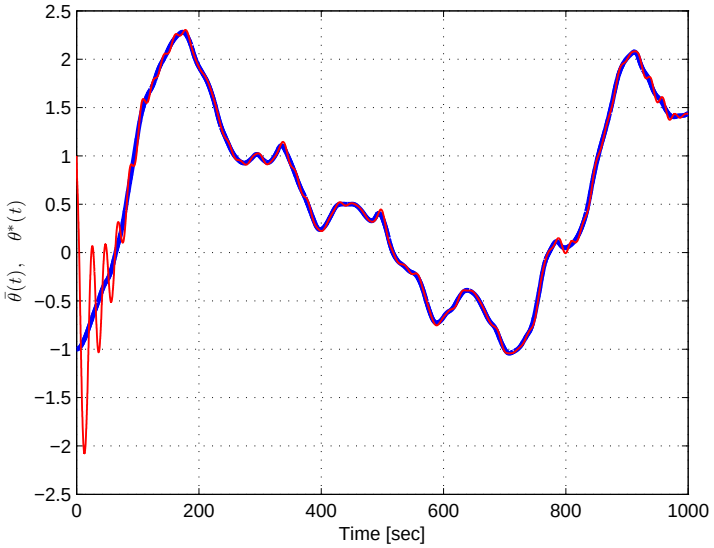

Figure 3.9: *The optimal trajectory tracking of the proposed RISE extremum seeking control method. The optimal variable $\theta^*(t)$ is shown in blue while the generated variable $\bar{\theta}(t)$ is shown in red.*

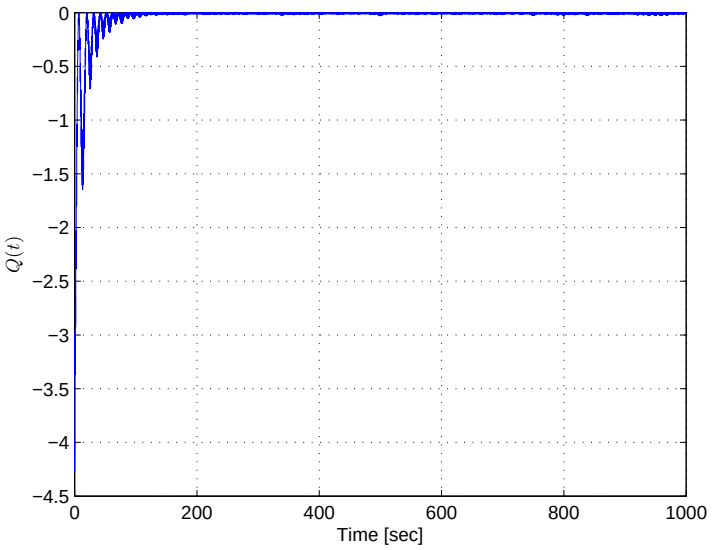

Figure 3.10: *The values of the cost function Q as a function of time, generated by the proposed robust extremum seeking control method.*

Chapter 4

Maximization of Power Capture in a Variable Speed Wind Turbine

4.1 Introduction

Early results on maximizing the power capture can be found in Xin 1997. One drawback of the method proposed there is that the optimal operating point is assumed to be known. The most used maximum power point tracking algorithms in the literature are those introduced in Datta and Ranganathan 2003, and Koutroulis and Kalaitzakis 2006, where several numerical techniques, comparisons, and decisions are to be made in order to estimate the optimal operation conditions. Johnson *et. al.* proposed a nonlinear controller (Johnson 2004, Johnson et al. 2006, and Johnson et al. 2004) where a control gain is adaptively tuned based on an estimation of the captured power. This approach had an adaptation on the order of hours and a convergence time on the order of days. To maximize wind energy captured in variable speed wind turbines at low to medium wind speeds, a robust control strategy is presented in Iyasere et al. 2008. The proposed strategy simultaneously controls the blade pitch and tip speed ratio, via the rotor angular speed, to an optimal point at which the power coefficient is maximum. The control method allows for aerodynamic rotor power maximization without the restrictions of exact wind turbine model knowledge. The proposed tracking method in Pan et al. 2008 combines the ideas of sliding mode control (SMC) and extremum seeking control (ESC). The only input needed in this method is the output active

power of the generator. It avoids some difficult problems in traditional tracking algorithms, such as measuring the wind velocity, the need of the wind-turbine model and parameters, and detecting the gradient of power versus rotor speed.

The extremum seeking strategy proposed in Krstic and Wang 2000 has recently been used for the maximum power point tracking problem. For MPPT problem in solar energy systems, the ESC method is experimentally tested (Brunton et al. 2009). The method shows a remarkable improvement in comparison with the previous methods for the same problem. For wind turbines, the power maximization problem is addressed in Creaby et al. 2009 based on similar extremum seeking control strategy. This paper seeks to find the optimal control torque while only measurements of power are available. However, some instabilities were observed due to variation in the mapping (Chen et al. 2010). To compensate for the variations of the mapping, Chen et al. 2010 considered input and sensor transfer functions in the ESC control loop and provided a robustness analysis.

In this chapter, the RISE extremum seeking method proposed in Chapter 3 is applied to design a maximum power point algorithm for wind turbines. The aerodynamic effect of the wind is considered as an unstructured uncertainty. This also addresses other uncertainties of the modeling. A strategy is provided to compute a filtered signal of the power, which is then employed in the control loop. Hence, the proposed controller does not need any wind or power measurements. The optimal point is assumed unknown and to be time-varying. As a consequence, the control algorithm is very robust in respect to any uncertainty in the modeling and measurement process.

4.2 Wind Turbine Modeling

4.2.1 Dynamic Model of a Variable Speed Wind Turbine

Several models have been proposed for wind turbines. The simplest one, a 1DOF model, is used in this thesis. The 1DOF dynamic model of the wind turbine is (Johnson et al. 2006, Iyasere et al. 2008)

$$J\dot{\omega} = -b\omega - \tau_c + \tau_{aero} \tag{4.1}$$

where ω is the rotor speed, J is the net rotating inertial, b is the net damping coefficient, τ_{aero} is the wind torque, and τ_c is the control torque.

The torque generated from the wind times the angular velocity is the captured wind power, namely,

$$P_{cap} = \tau_{aero}\omega. \tag{4.2}$$

At steady state conditions, the captured power has the following relation to the wind velocity

$$P_{cap} = \frac{1}{2} c_p(\lambda, \beta)\, \rho A v^3, \tag{4.3}$$

where v is wind velocity and λ is tip-speed ratio defined as

$$\lambda \triangleq \frac{\omega R}{v}. \tag{4.4}$$

In the above relations R is the length of the blades which have the pitch angle β, A is the area swept by the blades and ρ is the air density. In Equation (4.3), the power coefficient $c_p(\lambda, \beta)$ is a function of the tip-speed ratio and the pitch angle and determines the efficiency of power capture. The objective of maximum power point tracking algorithms is to maximize this coefficient.

In this section we assume that neither the wind velocity nor the power coefficient are measurable. In addition, we are interested in the case that the wind velocity varies through time. Hence, the maximum power point tracking problem in this case will be an extremum seeking control problem where both the optimal operating point and the maximum power capture are time-varying.

4.2.2 Discussions on Power Coefficient Function

The power coefficient function has a unique maximum in a wide range of tip speed ratio and blade pitch angle. A typical c_p mapping is shown in Fig. 4.1 (Iov et al. 2004). According to this surface, the optimal values are $\lambda^* = 7.8$, $\beta^* = -1^\circ$, $c_p^* = 0.4727$.

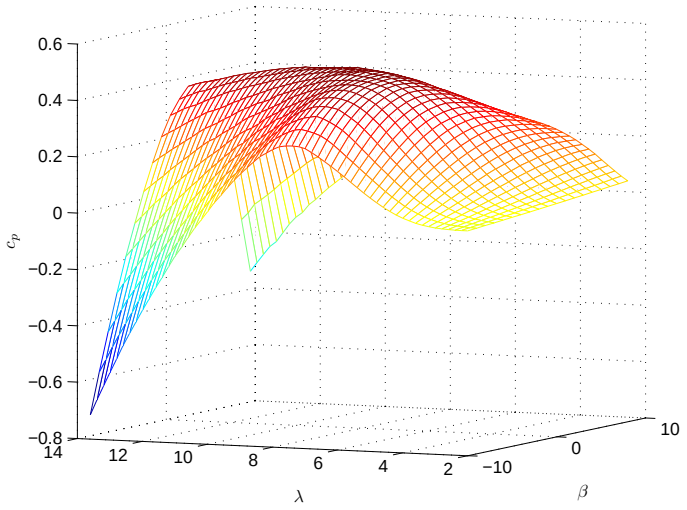

Figure 4.1: *The power coefficient c_p surface as a function of the tip speed ratio λ and pitch angle β.*

There also exists some analytic expressions for approximation of the $c_p(\lambda, \beta)$ mapping. For example, Agarwal et al. 2010 used the below expression to develop a novel rapid MPPT algorithm.

$$c_p(\lambda, \beta) = c_0 \left(\frac{c_1}{\lambda_i} - c_2\beta - c_3\beta^{\gamma_1} - c_4 \right) e^{-\gamma_2/\lambda_i}, \tag{4.5}$$

where

$$\lambda_i = \left(\frac{1}{\lambda - c_5\beta} - \frac{c_6}{\beta^3 + 1} \right)^{-1}, \tag{4.6}$$

and

$$\begin{aligned} c_0 &= 0.73,\ c_1 = 151,\ c_2 = 0.58,\ c_3 = 0.002, \\ c_4 &= 13.2,\ c_5 = 0.02,\ c_6 = 0.003, \\ \gamma_1 &= 2.14,\ \gamma_2 = 18.4. \end{aligned}$$

The optimal values for map (4.5) are $\beta^* = 0,\ \lambda^* = 7.054,\ c_p^* = 0.44$. For $\beta = 0$, the Eq. (4.5) becomes

$$c_p(\lambda) = c_0 \left(\frac{c_1}{\lambda} - c_4 \right) e^{-\gamma_2/\lambda}. \tag{4.7}$$

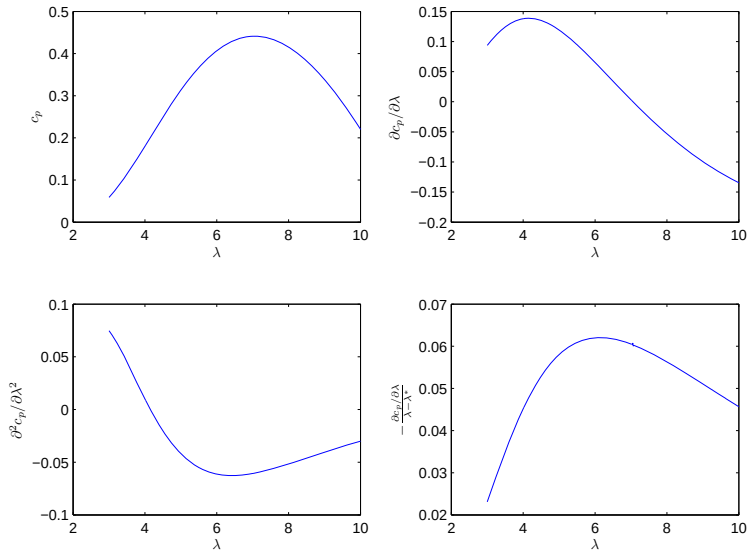

Figure 4.2: *Characteristics of c_p function.*

Using the expression in (4.7), the values of c_p, $\frac{\partial c_p}{\partial \lambda}$, $\frac{\partial^2 c_p}{\partial \lambda^2}$, and $-\frac{\partial c_p/\partial \lambda}{\lambda-\lambda^*}$ are calculated for $3 \leq \lambda \leq 10$ and plotted in Fig. 4.2. Note that even though $\frac{\partial^2 c_p}{\partial \lambda^2}$ is both positive and negative, $-\frac{\partial c_p/\partial \lambda}{\lambda-\lambda^*}$ is strictly positive for $3 \leq \lambda \leq 10$.

4.3 Active Control Methods of Wind Turbines

4.3.1 Classic Control Methods for Active Power Control

The power capture in Eq. (4.3) can be further manipulated to get the following form.

$$P_{cap} = \frac{1}{2} c_p(\lambda, \beta) \rho \pi R^2 v^3 \tag{4.8}$$

$$= \frac{1}{2} \frac{c_p(\lambda, \beta)}{\lambda^3} \rho \pi R^5 \omega^3 = \kappa(\lambda, \beta) \omega^3, \tag{4.9}$$

where the new variable $\kappa(\lambda, \beta)$ is defined as

$$\kappa \triangleq \frac{1}{2} \rho \pi R^5 \frac{c_p(\lambda, \beta)}{\lambda^3}. \tag{4.10}$$

In terms of κ, the aerodynamic torque τ_{aero} can be written as

$$\tau_{aero} = \kappa\omega^2. \tag{4.11}$$

Consider the case where the pitch angle is fixed. In this case, assume that the optimal value of κ, i.e.,

$$\kappa^*(\lambda) = \frac{1}{2}\rho\pi R^5 \frac{c_p(\lambda^*)}{\lambda^{*3}} \tag{4.12}$$

is known. By selecting the control input $\tau \triangleq b\omega + \tau_c$ as

$$\tau = \kappa^*(\lambda)\omega^2, \tag{4.13}$$

the value of ω will move to the point where $\lambda = \lambda^*$ (see Johnson et al. 2004). The problem with this method is that the optimal value κ^* must be known. However, in most of the practical cases it is not possible to have such information.

For practical applications, Johnson et al. 2004 proposed the controller

$$\tau = K\omega^2 \tag{4.14}$$

where the control gain K is adaptively updated so that the average captured power is maximized.

By selecting the controller (4.14), the system (under some conditions) goes to the point where

$$\kappa(\lambda) = K. \tag{4.15}$$

In Figure (4.3), the mapping $\kappa(\lambda) \rightarrow c_p(\lambda)$ is plotted for $3 \leq \lambda \leq 10$ using the equation (4.7) and $\frac{1}{2}\rho\pi R = 1$.

4.3.2 RISE Control Algorithm for Robust Speed Tracking

In rotor speed tracking problem, it is desired to design control laws for the input torque such that the rotor speed tracks a desired trajectory $\omega_d(t)$. However, as can be seen in Eq. (4.1), the rotor speed is influenced by the aerodynamic torque. Since, there is no authority

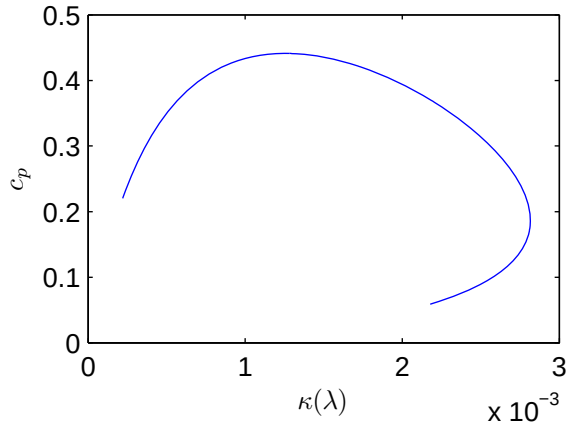

Figure 4.3: $c_p(\lambda) - \kappa(\lambda)$ *curve.*

over the aerodynamic impact of the wind, the rotor speed tracking control must necessarily be robust to aerodynamic torque. Considering the aerodynamic torque as an unstructured disturbance, Hawkins 2010 and Iyasere et al. 2008 used RISE method to design the robust speed tracking algorithm. The design procedure is as follows.

To facilitate the controller design, equation (4.1) is rewritten as the following

$$\dot{\omega} = -\frac{k}{J}\omega - \frac{1}{J}\tau_c + \frac{1}{J}\tau_{aero}, \tag{4.16}$$

which can further be simplified to get the following form

$$\dot{\omega} = u + f(t), \tag{4.17}$$

where

$$u \triangleq -\frac{k}{J}\omega - \frac{1}{J}\tau_c, \;\; f(t) \triangleq \frac{1}{J}\tau_{aero}. \tag{4.18}$$

An identifier is proposed as

$$\hat{f}(t) = (b_1 + 1)\left(\tilde{\omega}(t) - \tilde{\omega}(0)\right) + \int_0^t \alpha(b_1 + 1)\tilde{\omega}(\tau) + b_2 sgn(\tilde{\omega}(\tau))d\tau, \tag{4.19}$$

where

$$\tilde{\omega} \triangleq \omega - \omega_d, \tag{4.20}$$

$\alpha > \frac{1}{2}$, and b_1 and b_2 are two big positive gains. By selecting the control input u as

$$u = \dot{\omega}_d - \hat{f}(t), \tag{4.21}$$

it can be proved that this control guarantees a semi-global asymptotic stability (See Hawkins 2010 or Iyasere et al. 2008 for similar proof).

4.4 MPPT Control Loop Development

As indicated earlier this thesis uses the RISE extremum seeking for the maximum power point tracking problem in a wind turbine. To complete the control loop development, three components of the control loop must be chosen. The first one is the searching variable θ. It must be determined which parameter is going to be updated to reach the optimal value. The next component is employing the internal stabilization method so that the rotor speed of the wind turbine is regulated corresponding to the searching variable θ. The last remaining component is the output. The captured power is usually a good candidate for this purpose. However, there is often no direct measurements of the captured power available for the feedback purpose. Therefore, an estimation or a filtered signal might be used.

In this thesis, the searching variable θ is selected as the desired rotor speed ω_d. Therefore, the control loop will be the following. A sinusoidal perturbation is added to the signal $\bar{\omega}_d$. Then, an appropriate control torque is applied to the wind turbine to track the desired rotor speed. The generated power is then fed into the gradient estimation unit. The estimated gradient is then used in the RISE gradient search to update the desired rotor speed. With an appropriate arrangement of the control loop parameters, the desired rotor speed will converge to the optimal rotor speed at which maximum power is generated.

The internal stabilization control method is chosen as the RISE robust tracking strategy described in Section 4.3.2. It should be noted that the aim of the internal stabilization is to make the input-to-output mapping have a quasi-static dynamical characteristic. Therefore, the control gains should be selected so that the tracking task is performed relatively much

faster than the adaptation process. In practical application, the speed control of wind turbine blades is restricted by the large inertia of the blades and limited acceptable control torque. However, in this thesis, these practical limitations are not considered.

As discussed earlier, the desired output for maximization is the captured power. Hence, a suitable choice of output can be $Q = f\omega$. However, since the measurements of f are not available, it is not possible to select $Q = f\omega$ as the measurable output. In the subsequent analysis it is shown that

$$y = \frac{p}{s+p} f\omega \tag{4.22}$$

is measurable where p is a filter constant.

Lemma 4.1. *According to dynamic model (4.17) for a variable speed wind turbine, it is possible to obtain the following output*

$$y = \frac{p}{s+p} P_{cap} \tag{4.23}$$

only based on the measurements of the rotor speed and the control input measurements.

Proof. Multiplying both sides of (4.17) by ω, we will get

$$\dot{\omega}\omega = f\omega + u\omega \tag{4.24}$$

which is equivalent to

$$\frac{d}{dt}\left(\frac{1}{2}\omega^2\right) = f\omega + u\omega. \tag{4.25}$$

Writing the above equation in Laplace domain and multiplying both sides by $\frac{p}{s+p}$ results in

$$\begin{aligned} \frac{p}{s+p} f\omega &= \frac{ps}{s+p}(\frac{1}{2}\omega^2) - \frac{p}{s+p} u\omega \\ &= \frac{p}{2}\omega^2 - \frac{p}{s+p}(\frac{p}{2}\omega^2 + u\omega). \end{aligned} \tag{4.26}$$

Since the rotor speed ω and the control input u, as designed in Eq. 4.21, are measurable, $y = \frac{p}{s+p} f\omega$ is measurable. □

Component	Selection
Searching Variable	ω_d
Internal Controller	RISE Stabilizer
Output	$\frac{1}{s+p} f\omega$

Table 4.1: *MPPT control loop components.*

Remark 7. *The filtering constant p in (4.23), can be selected to have any positive value. Considering the nature of the output power of a wind turbine, p should be selected small enough to get rid of the high frequency variations caused by wind turbulence and, at the same time, big enough to avoid losing any generated power during the optimization process.*

Table 4.1 shows the control loop component selection.

4.5 Simulation Results

In this section, the developed MPPT algorithm in Section 4.4 is tested through numerical simulations. The software package used for the simulation purpose is the "*Wind Turbine Blockset V.3*" for Simulink created by Iov et. al. (see Iov et al. 2004). This software provides several blocks which can be easily used in Simulink/MATLAB. For the simulations in this section, the "Wind Model SB-1" block and the "Wind Turbine Rotor Variable Pitch" block are used. The "Wind Model SB-1" block generates the wind signal. The wind signal can be specified by the average wind velocity and the turbulence percentage. The "Wind Turbine Rotor Variable Pitch" is used for simulation of the wind turbine. The inputs to this block are the pitch angle, rotor speed, and the wind velocity. The block uses a look-up table for the $c_p(\lambda, \beta)$, shown in Figure (4.1), to compute the generated torque. The generated torque is then used in the 1DOF model (4.1). The parameters which have been used in the simulation are shown in Table 4.2.

4.5.1 Simulation Results

Three simulation results are provided to demonstrate the performance of the RISE extremum seeking algorithm. In the simulations, it is assumed that the wind has 10% turbulence. The

Parameter	Symbol	Value
Net Rotating Inertia	J	10^5 kg m^2
Net Damping Ratio	b	0 kg m^2 s^{-1}
Blade Pitch Angle	β	-1°
Blade Radius	R	40 m
Average Wind Velocity	$\bar{v}$	10 m s^{-1}
Air Density	ρ	1.25 kg m^{-3}

Table 4.2: *Wind turbine parameter setup for simulation.*

wind velocity profile is shown in Figure (4.4).

Simulation 1. RISE ESC for desired rotor speed adaptation. The RISE extremum seeking algorithm proposed in Chapter 3 is used to make the desired rotor speed $\bar{\omega}_d(t)$ to achieve the optimal value $\omega^*(t) = \frac{\lambda^* R}{v_{wind}}$. The only measurable data is $\omega(t)$. In Figure (4.5), the generated $\bar{\omega}_d$ and the actual optimal value $\omega^*(t) = \frac{\lambda^* R}{v_{wind}}$ are plotted for the proposed RISE extremum seeking algorithm. The actual and the maximum possible values for the captured power are depicted in Figure (4.6). It can be observed that the captured power is very close to the maximum possible value using the RISE extremum seeking method. In Figure (4.7), the aerodynamic torque and the control torque are presented.

Simulation 2. Classic ESC for desired rotor speed adaptation. Classic ESC method is used for adaptation for the optimal $\bar{\omega}_d$. In Figure (4.8), the generated $\bar{\omega}_d$ and the actual optimal value $\omega^*(t) = \frac{\lambda^* R}{v_{wind}}$ are plotted. It can be easily observed that the classic ESC method is not very successful in identifying and tracking the optimal rotor speed. The justification is that the optimal value is time-varying, and therefore, cannot be tracked well using classic ESC method.

Simulation 3. Classic ESC for control gain adaptation. The optimal control gain is constant. The classical extremum seeking algorithm is utilized for finding the optimal control gain K in $\tau_c = K\omega^2$. According to Eq. (4.12), the parameters values in Table (4.2),

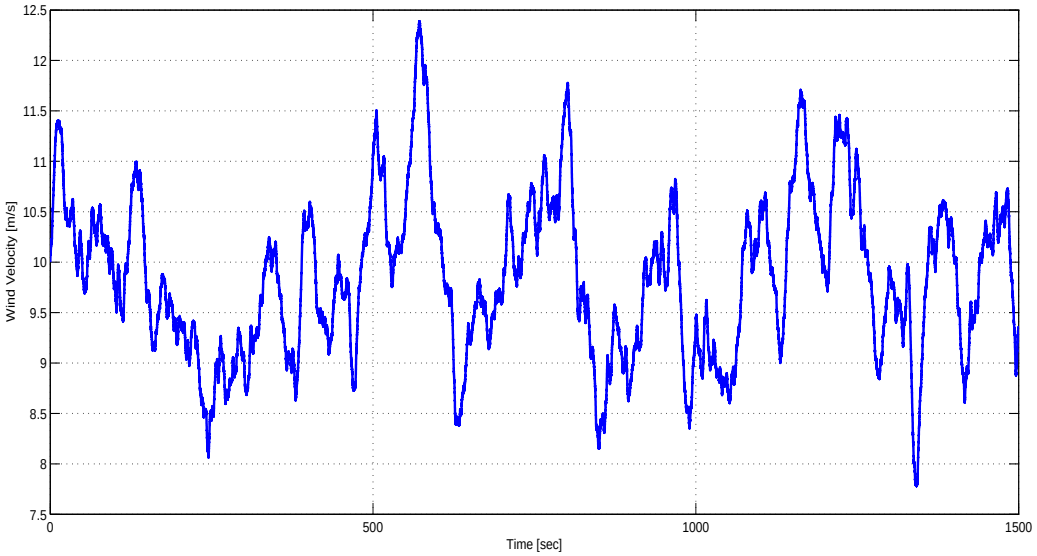

Figure 4.4: *The wind velocity profile as a function of time with* 10% *turbulence.*

and the c_p curve, the optimal value for the control gain is

$$\begin{aligned} K^* &= \frac{1}{2}\rho\pi R^5 \frac{c_p(\lambda^*)}{\lambda^{*3}} \\ &= .5 \times 1.25 \times \pi \times 40^5 \times \frac{.4727}{7.8^3} = 200,277\,\mathrm{N\,m^2\,sec^2}\,. \end{aligned}$$

In Figure (4.9), the obtained control gain is shown. Since the optimal point in this case is time-invariant, the classic ESC method can reach the optimal value. The captured power with this method and the maximum capturable power are depicted in Figure (4.10).

4.6 Concluding Remarks

In Table 4.3, some adaptation strategies for the MPPT problem in wind turbines are listed. The peak-seeking algorithms in the first three references are based on numerical optimization methods. The methods used in these references necessarily require time-invariant mappings. Since the power map in a wind turbine is by nature time-varying, some approaches have been devised for successful implementation of the MPPT algorithms. Specifically, Johnson 2004

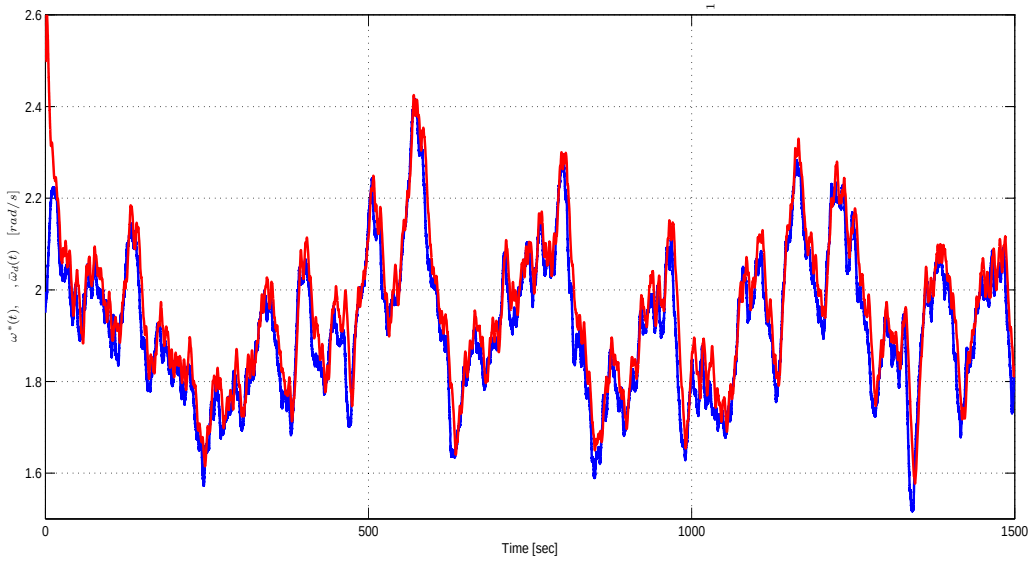

Figure 4.5: *The actual optimal value $\omega^*(t)$ (blue) and the generated $\bar{\omega}_d$ (red) by the proposed RISE extremum seeking algorithm.*

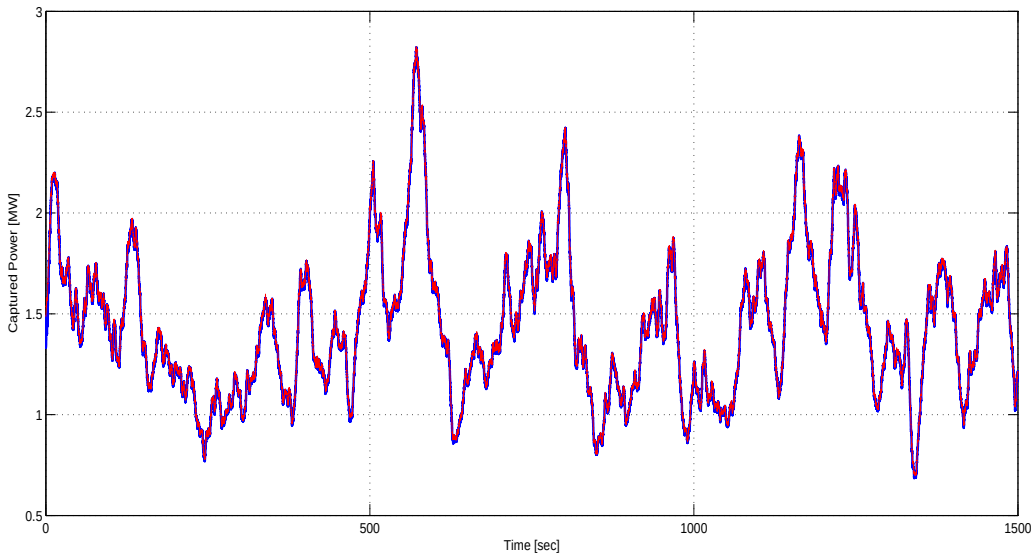

Figure 4.6: *Maximum possible power capture versus the actual captured power using the RISE extremum seeking algorithm. The captured power is shown in red and the maximum possible value is plotted in blue.*

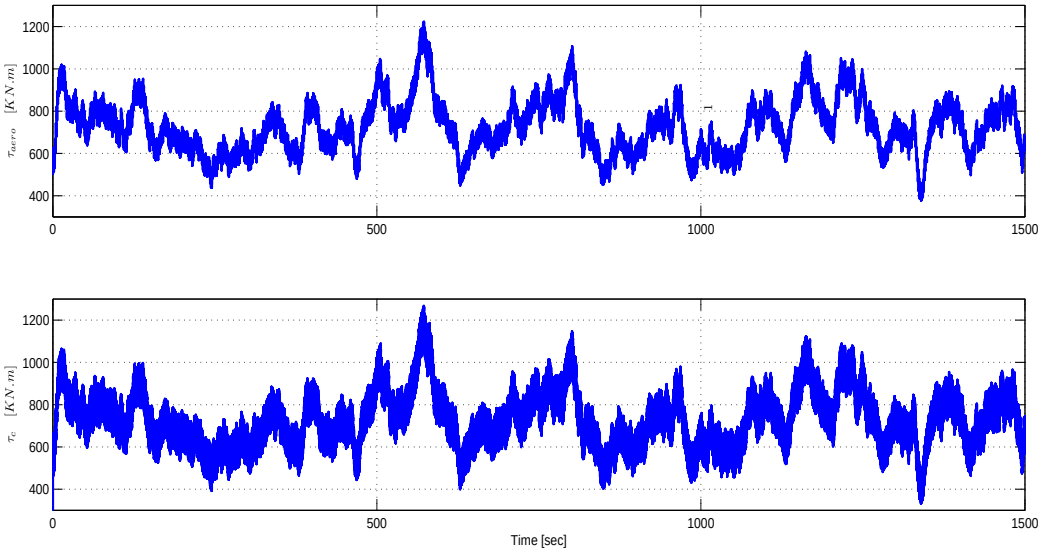

Figure 4.7: *The aerodynamic torque and the control torque input using the RISE extremum seeking algorithm.*

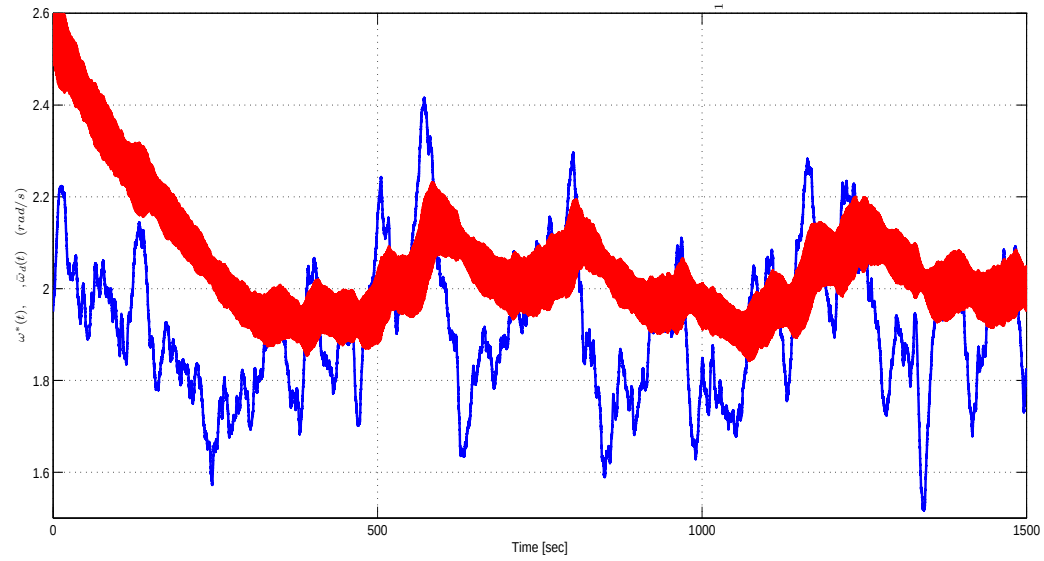

Figure 4.8: *The actual optimal value $\omega^*(t)$ (blue) and the generated $\bar{\omega}_d$ (red) by a classic extremum seeking algorithm.*

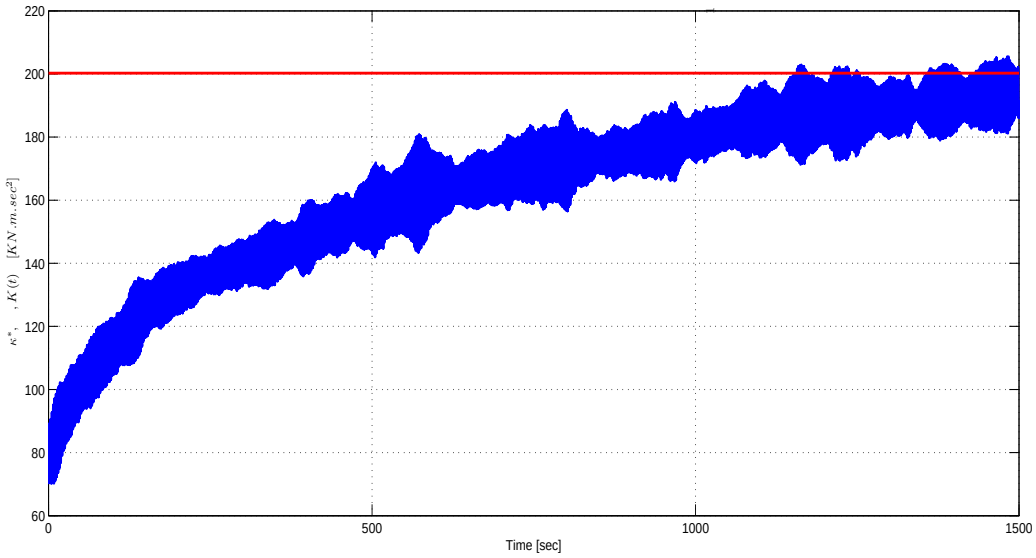

Figure 4.9: *Control gain adaptation using the classic ESC method. The red line represents the optimal value.*

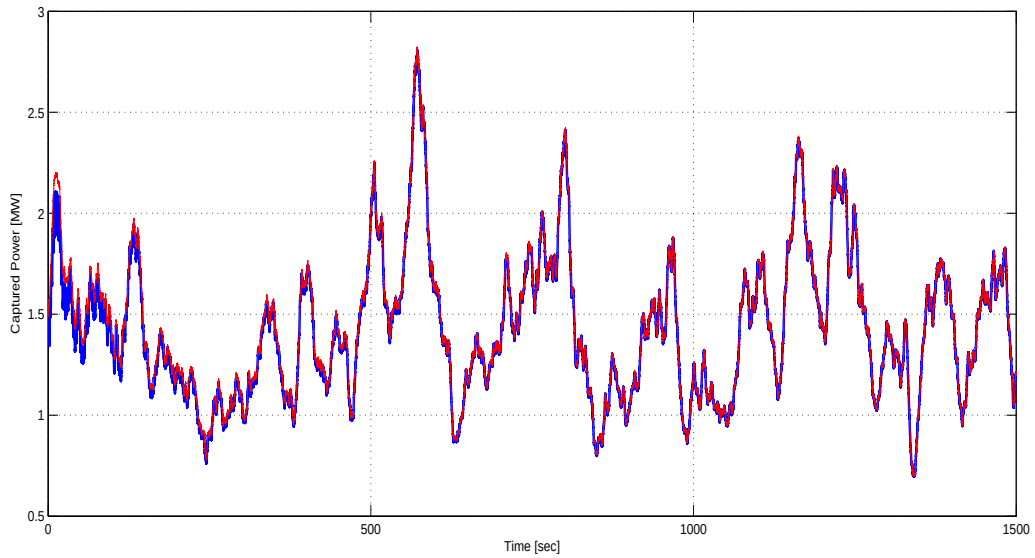

Figure 4.10: *Maximum possible power capture versus the actual captured power using classic ESC method for gain adaptation. The captured power is shown in red and the maximum value is plotted in blue.*

calculated the average of the long term power capture, and then used the averaged value in the steepest descent algorithm. In this way, the mapping which is used for the numerical search is almost time-invariant. Therefore, the numerical optimization operates properly. Hawkins 2010 assumed that the wind velocity is measurable and instead of the power map, the power coefficient c_p map was used. The power coefficient map is time-invariant so the numerical optimization can be successfully employed. Iyasere et al. 2008 provided results for the case where the wind velocity is constant. If the wind speed is constant, the power map is time-invariant which allows the Powel's method to be used.

The MPPT algorithms in Creaby et al. 2009, Chen et al. 2010, and the current work are based on continuous time extremum seeking control methods. The ESC method which is used in Creaby et al. 2009 is for time-invariant mappings. As discussed earlier, this method performs satisfactorily for time-varying mappings if the time variation of the mapping is much slower than the adaptation dynamics. However, in a wind turbine, the time variations of the system are considerable and should be properly handled. As a consequence, unstable results are observed in Creaby's method (see Chen et al. 2010). Chen et al. 2010 considered dynamic mapping for power maximization in wind turbines. Making use of the ESC method enhanced the performance.

As reported in Chapter 2, an extremum seeking control method is developed for mappings where the optimal point and the optimal value are functions of time in Krstic 2000. However, the structure of the variation by time must be known. Because of the turbulent nature of wind, it is not possible to propose an accurate model for the variations of the wind. In this thesis, the variation of the mapping is considered completely unknown. The power mapping is allowed to be varying by time in a very general form. However, we assume that the optimal point is changing smoothly. Therefore, sudden changes in wind speed and persistent high frequency variations of the wind might deteriorate the performance of the proposed MPPT algorithm.

Mapping	**Reference**	**Searching Method**	**Application Limitation**
$K \rightarrow P$	Johnson et al. 2006	Steepest descent	Very slow convergence
$(\lambda, \beta) \rightarrow c_p$	Hawkins 2010	Switching step search	Wind velocity measurement
$(\omega, \beta) \rightarrow P$	Iyasere et al. 2008	Powel's method	Constant wind velocity
$(\tau_c, \beta) \rightarrow P$	Creaby et al. 2009	ESC	Instability of results due to mapping variations.
$\tau_c \rightarrow P$	Chen et al. 2010	ESC with mapping dynamics	
$\omega \rightarrow P$	Current work	RISE ESC	Complicated control loop.

Table 4.3: *Peak-seeking control methods for MPPT problem in wind turbines.*

Chapter 5

Conclusion and Future Work

5.1 Summary and Conclusion

In this thesis, the maximum power point tracking (MPPT) problem in wind turbines is addressed. For a given wind velocity, the amount of the captured power is dependent on the rotor speed. There is an optimal rotor speed at which the captured power is maximum for the given wind velocity. This optimal rotor speed is dependent on the wind velocity. In practice, the wind field is constantly changing. As a consequence, the optimal operating point of the wind turbine is also varying. Finding the optimal point is challenging, specifically due to several technological limitations for direct measurements of the wind velocity. In this thesis, an MPPT algorithm is proposed to identify and track the optimal rotor speed trajectory without any measurements of the wind velocity. Furthermore, direct measurements of the captured power are not essential for the implementation of the MPPT loop.

For designing the proposed MPPT algorithm, a new extremum seeking method is used. In an extremum seeking algorithm, the system states are derived to a point where a mapping is at its extremum (maximum or minimum) value. All the existing extremum seeking algorithms are for the systems where the mapping is time-independent. If a mapping is time-dependent, then the time-variation must be very slow or the structure of the variation must be known. The extremum seeking algorithm developed in this thesis does not make such assumptions about the mapping variations. The mapping is allowed to be time-dependent

in a very general form. The optimal point is assumed to be varying smoothly over time.

The extremum seeking control method in this thesis basically consists of two separate components, i.e., 1) gradient estimation and 2) RISE gradient search. The gradient estimation is realized through adding a sinusoidal perturbation to the searching signal and then demodulating the measured output. A delay-based strategy is developed to extract the gradient. The estimated gradient signal is then fed into the RISE gradient search method. The developed RISE gradient search method is proved to move the searching signal toward the optimal value. Some simulations are provided to show the performance of the proposed extremum seeking algorithm.

The proposed RISE extremum seeking method is applied to the maximum power point tracking problem in wind turbines. The simulation results show that the designed MPPT algorithm can keep the wind turbine system operating at the optimal rotor speed. The performance is then compared with classic extremum seeking methods for rotor speed adaptation and control gain adaptation.

5.2 Suggestions for Future Work

The RISE extremum seeking algorithm which is introduced in this thesis is proved for single dimensional search. It will be interesting to extend the results to cases where the searching signal is multi-dimensional. In this report, each component of the extremum seeking control loop is designed based on the assumption of the separation of time-scale. The output of each component is consistent with the input requirements of the next component. However, the analysis for quantifying the separation of time-scales are not presented. To obtain this, the closed-loop system should be analyzed as a whole. Another assumption of the proposed extremum seeking algorithm is that the mapping is static. Therefore, the method can only be applied to quasi-static mappings. Enhancing the capabilities of the RISE extremum seeking for dynamic mappings can be a topic for future work.

All the extremum seeking methods primarily rely on introducing dither signals in the

control loop. In practice, the frequency of the dither signal might induce fatigue in the turbine structure. As a result, this fact can be considered as a drawback of these methods. The variations of the wind velocity due to turbulence has already been used for the MPPT problem (Munteanu et al. 2008). The idea is that when the wind velocity changes, the tip speed ratio will also change. This could be used as a natural perturbation to the searching signal (here, the tip speed ratio). The problem with this method is that a reliable measurement of the wind velocity must be available. Another approach which might be useful is to use the persistent tower vibrations in a wind turbine as a dither signal.

Bibliography

Thomas Ackermann, Göran Andersson, and Lennart Söder. Distributed generation: a definition. *Electric Power Systems Research*, 57(3):195 – 204, 2001.

V. Agarwal, R.K. Aggarwal, P. Patidar, and C. Patki. A novel scheme for rapid tracking of maximum power point in wind energy generation systems. *Energy Conversion, IEEE Transactions on*, 25(1):228 –236, 2010.

Kartik B. Ariyur and Miroslav Krstic. *Real-Time Optimization by Extremum-Seeking Control*. Wiley-Interscience, A John Wiley & Sons, Inc, 2003.

Kartik B. Ariyur and Miroslav Krstic. Slope seeking: a generalization of extremum seeking. *International Journal of Adaptive Control and Signal Processing*, 18(1):1–22, 2004.

S.L. Brunton, C.W. Rowley, S.R. Kulkarni, and C. Clarkson. Maximum power point tracking for photovoltaic optimization using extremum seeking. In *Photovoltaic Specialists Conference (PVSC), 2009 34th IEEE*, pages 13 –16, 2009.

Quan Chen, Yaoyu Li, Zhongzhou Yang, John E. Seem, and Justin Creaby. Self-optimizing robust control of wind power generation with doulby-fed induction generator. In *Dynamic Systems and Control Conference*, 2010.

Z. Chen and E. Spooner. Grid power quality with variable speed wind turbines. *Energy Conversion, IEEE Transactions on*, 16(2):148 –154, jun 2001.

Debora Coll-Mayor, Rodrigo Picos, and Eugeni Garcia-Moreno. State of the art of the virtual utility: the smart distributed generation network. *International Journal of Energy Research*, 28(1):65–80, 2004.

Justin Creaby, Yaoyu Li, and John E. Seem. Maximizing wind turbine energy capture using multivariable extremum seeking control. *Wind Engineering*, 33(4):361–387, 2009.

Zhi dan Zhong, Hai bo Huo, Xin jian Zhu, Guang yi Cao, and Yuan Ren. Adaptive maximum power point tracking control of fuel cell power plants. *Journal of Power Sources*, 176(1): 259 – 269, 2008.

R. Datta and V.T. Ranganathan. A method of tracking the peak power points for a variable speed wind energy conversion system. *Energy Conversion, IEEE Transactions on*, 18(1): 163 – 168, mar 2003.

M. Guay and T. Zhang. Adaptive extremum seeking control of nonlinear dynamic systems with parametric uncertainties. *Automatica*, 39(7):1283–1293, 2003.

T.J. Hammons. Integrating renewable energy sources into european grids. *International Journal of Electrical Power & Energy Systems*, 30(8):462 – 475, 2008.

T. Hawkins. Maximization of power capture in wind turbines using robust estimation and lyapunov extremum seeking control. Master's thesis, Kansas State University, 2010.

F Iov, AD Hansen, P Sorensen, and F Blaabjerg. Wind turbine blockset in matlab/simulink general overview and description of the models. Technical report, Aalborg University, Denmark, 2004.

E. Iyasere, M. Salah, D. Dawson, and J. Wagner. Nonlinear robust control to maximize energy capture in a variable speed wind turbine. In *American Control Conference*, pages 1824 –1829, 2008.

Kathryn E. Johnson, Lee J. Fingersh, Mark J. Balas, and Lucy Y. Pao. Methods for increasing region 2 power capture on a variable-speed wind turbine. *Journal of Solar Energy Engineering*, 126(4):1092–1100, 2004.

K.E. Johnson. Adaptive torque control of variable-speed wind turbines. Technical report, National Renewable Energy Laboratory, August 2004.

K.E. Johnson, L.Y. Pao, M.J. Balas, and L.J. Fingersh. Control of variable-speed wind turbines: standard and adaptive techniques for maximizing energy capture. *Control Systems Magazine, IEEE*, 26(3):70 – 81, june 2006.

H. K. Khalil. *Nonlinear Systems*. Prentice-Hall, Inc., New Jersey, 3 edition, 2002.

E. Koutroulis and K. Kalaitzakis. Design of a maximum power tracking system for wind-energy-conversion applications. *Industrial Electronics, IEEE Transactions on*, 53(2):486 – 494, april 2006.

M. Krstic. Performance improvement and limitations in extremum seeking control. *Systems & Control Letters*, 39(5):313–326, 2000.

Miroslav Krstic and Hsin-Hsiung Wang. Stability of extremum seeking feedback for general nonlinear dynamic systems. *Automatica*, 36(4):595 – 601, 2000.

J.H. Laks, L.Y. Pao, and A.D. Wright. Control of wind turbines: Past, present, and future. In *American Control Conference*, pages 2096 –2103, june 2009.

R.H. Lasseter and P. Paigi. Microgrid: a conceptual solution. In *Power Electronics Specialists Conference, 2004. PESC 04. 2004 IEEE 35th Annual*, volume 6, pages 4285–4290 Vol.6, June 2004.

C. Makkar, G. Hu, W. G. Sawyer, and W. E. Dixon. Lyapunov-based tracking control in the presence of uncertain nonlinear parameterizable friction. *IEEE Transactions on Automatic Control*, 52(10):1988–1994, Oct. 2007.

C. Manzie and M. Krstic. Extremum seeking with stochastic perturbations. *IEEE Transactions on Automatic Control*, 54(3):580 –585, march 2009.

I. Munteanu, A.I. Bratcu, N.A. Cutululis, and E. Ceanga. *Optimal control of wind energy systems: towards a global approach*. Springer Verlag, 2008. ISBN 1848000790.

Tinglong Pan, Zhicheng Ji, and Zhenhua Jiang. Maximum power point tracking of wind energy conversion systems based on sliding mode extremum seeking control. In *IEEE Energy 2030 Conference*, pages 1 –5, nov. 2008.

L.Y. Pao and K.E. Johnson. A tutorial on the dynamics and control of wind turbines and wind farms. In *American Control Conference*, pages 2076 –2089, june 2009.

P.M. Patre, W. MacKunis, C. Makkar, and W.E. Dixon. Asymptotic tracking for systems with structured and unstructured uncertainties. *Control Systems Technology, IEEE Transactions on*, 16(2):373 –379, 2008.

Mario Rabinowitz. Power systems of the future. *Power Engineering Review*, 20:4, 2000.

J.L. Rodriguez-Amenedo, S. Arnalte, and J.C. Burgos. Automatic generation control of a wind farm with variable speed wind turbines. *Energy Conversion, IEEE Transactions on*, 17(2):279 –284, jun 2002.

V. Salas, E. Olías, A. Barrado, and A. Lázaro. Review of the maximum power point tracking algorithms for stand-alone photovoltaic systems. *Solar Energy Materials and Solar Cells*, 90(11):1555 – 1578, 2006.

Y. Tan, D. Nesic, I.M.Y. Mareels, and A. Astolfi. On global extremum seeking in the presence of local extrema. *Automatica*, 45(1):245 – 251, 2009.

Y. Tan, W.H. Moase, C. Manzie, D. Nes andic and, and I.M.Y. Mareels. Extremum seeking from 1922 to 2010. In *Control Conference (CCC), 2010 29th Chinese*, pages 14 –26, 2010.

Ying Tan, Dragan Nesic, and Iven Mareels. On non-local stability properties of extremum seeking control. *Automatica*, 42(6):889 – 903, 2006.

Ying Tan, Dragan Nesic, and Iven Mareels. On the choice of dither in extremum seeking systems: A case study. *Automatica*, 44(5):1446 – 1450, 2008.

A.R. Teel and D. Popovic. Solving smooth and nonsmooth multivariable extremum seeking problems by the methods of nonlinear programming. In *American Control Conference*, volume 3, pages 2394 –2399 vol.3, 2001.

B. Xian, D. M. Dawson, M.S. de Queiroz, and J. Chen. A continuous asymptotic tracking control strategy for uncertain nonlinear systems. *IEEE Transactions on Automatic Control*, 49(7):1206–1211, July 2004.

M. Xin. *Adaptive Extremum Control and Wind Turbine Control*. PhD thesis, Informatics and Mathematical Modelling, Technical University of Denmark, DTU, Richard Petersens Plads, Building 321, DK-2800 Kgs. Lyngby, 1997.

R. Zavadil, N. Miller, A. Ellis, and E. Muljadi. Making connections [wind generation facilities]. *Power and Energy Magazine, IEEE*, 3(6):26–37, Nov.-Dec. 2005.

Appendix A

Appendix

Proof of (3.37-3.38).

Using the Mean Value Theorem, there exists a time $t' \in (\tau, t)$, where

$$\frac{d}{d\tau} Q_\theta|_{\tau=t'} = \frac{Q_\theta(t) - Q_\theta(\tau)}{t-\tau}. \tag{A.1}$$

Therefore, $Q_\theta(\bar{\theta}(\tau), \varrho(\tau))$ can be expressed as

$$Q_\theta(\bar{\theta}(\tau), \varrho(\tau)) = Q_\theta(\bar{\theta}(t), \varrho(t)) + \frac{d}{d\tau} Q_\theta|_{\tau=t'}(\tau - t). \tag{A.2}$$

Substituting for $Q_\theta(\bar{\theta}(\tau), \varrho(\tau))$, the following is ture

$$\begin{aligned}
&\frac{1}{2\pi}\int_{t-T}^{t} af Q_\theta(\bar{\theta}(\tau), \varrho(\tau)) \sin(\omega\tau + \psi)\sin(\omega\tau + \varphi)d\tau = \\
&\frac{1}{2\pi}\int_{t-T}^{t} af \left\{ Q_\theta(\bar{\theta}(t), \varrho(t)) + \dot{Q}_\theta(t')(\tau - t) \right\} \sin(\omega\tau + \psi)\sin(\omega\tau + \varphi)d\tau = \\
&\frac{1}{2\pi} Q_\theta(\bar{\theta}(t), \varrho(t)) \int_{t-T}^{t} af \sin(\omega\tau + \psi)\sin(\omega\tau + \varphi)d\tau + \epsilon_4(\cdot),
\end{aligned} \tag{A.3}$$

where

$$\epsilon_4(\cdot) = \frac{1}{2\pi}\dot{Q}_\theta(t') af \int_{t-T}^{t} (\tau - t)\sin(\omega\tau + \psi)\sin(\omega\tau + \varphi)d\tau. \tag{A.4}$$

The first integral term in (A.3) can be calulated as

$$\begin{aligned}
&\frac{1}{2\pi} Q_\theta(\bar{\theta}(t), \varrho(t)) \int_{t-T}^{t} af \sin(\omega\tau + \psi)\sin(\omega\tau + \varphi)d\tau = \\
&\frac{1}{2\omega} af \cos(\varphi - \psi) Q_\theta(\bar{\theta}, \varrho).
\end{aligned} \tag{A.5}$$

Based on (A.3) and (A.5) the following is concluded

$$\frac{1}{2\pi}Q_\theta(\bar{\theta}(t),\varrho(t))\int_{t-T}^{t} af\sin(\omega\tau+\psi)\sin(\omega\tau+\varphi)d\tau = \frac{1}{2\omega}af\cos(\varphi-\psi)Q_\theta(\bar{\theta},\varrho)+\epsilon_4(.). \tag{A.6}$$

Hence, the Eq. (3.37) is proved.

The integral term in (A.4) can be compouted as

$$\int_{t-T}^{t}(\tau-t)\sin(\omega\tau+\psi)\sin(\omega\tau+\varphi)d\tau = \frac{-\pi}{2\omega^2}\{\sin(2\omega t+\psi+\varphi)+2\cos(\varphi-\psi)\pi\}. \tag{A.7}$$

Based on (A.4) and (A.7), the error term $\epsilon_4(\cdot)$ can be expressed as

$$\epsilon_4(\cdot) = \frac{-\pi}{4\omega^2}\dot{Q}_\theta(t')af\{\sin(2\omega t+\psi+\varphi)+2\cos(\varphi-\psi)\pi\}. \tag{A.8}$$

According to Eq. (A.8) and Eq. (3.32),

$$\epsilon_4(\cdot) = \mathcal{O}(a\varepsilon\frac{1}{\omega^2}), \tag{A.9}$$

which is similar to Eq. (3.38). Hence the proof.